AD-A146 500 DERIVATION OF RECURSIVE DIGITAL FILTERS BY THE STEP-INVARIANT AND THE RAM.. (U) DEFENCE RESEARCH ESTABLISHMENT VALCARTIER (QUEBEC) A MORIN ET AL. 1/1

UNCLASSIFIED MAY 84 DREV-R-4325/84 F/G 12/1 NL

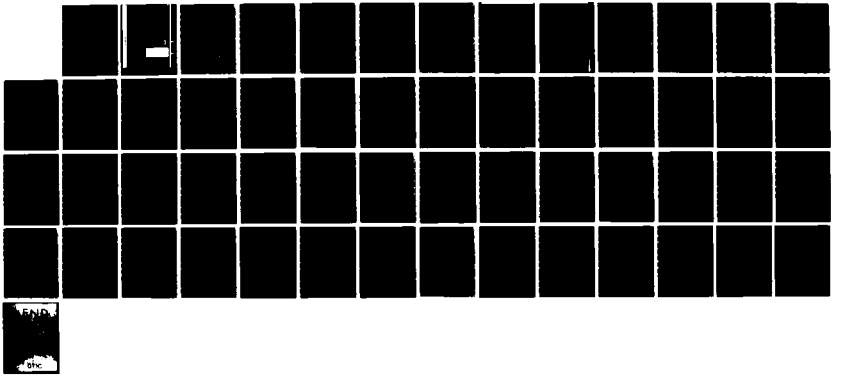

END

DTIC

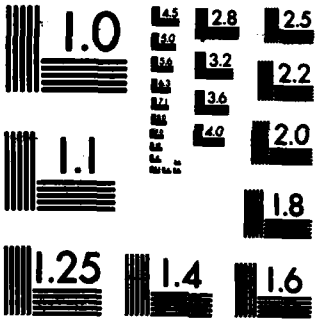
1.0
1.1
1.25
1.4
1.6
1.8
2.0
2.2
2.5
2.8
3.2
3.6
4.0
4.5

National Defence / Défense nationale

UNCLASSIFIED
UNLIMITED DISTRIBUTION

DREV REPORT 4325/84
FILE: 3621J-005
MAY 1984

CRDV RAPPORT 4325/84
DOSSIER: 3621J-005
MAI 1984

DERIVATION OF RECURSIVE DIGITAL FILTERS BY THE STEP-INVARIANT AND THE RAMP-INVARIANT TRANSFORMATIONS

A. Morin

P. Labbé

BUREAU - RECHERCHE ET DÉVELOPPEMENT
MINISTÈRE DE LA DÉFENSE NATIONALE
CANADA

RESEARCH AND DEVELOPMENT BRANCH
DEPARTMENT OF NATIONAL DEFENCE
CANADA

Canada

NON CLASSIFIÉ
DIFFUSION ILLIMITÉE

DERIVATION OF RECURSIVE DIGITAL FILTERS BY THE STEP-INVARIANT AND THE RAMP-INVARIANT TRANSFORMATIONS

by

A. Morin and P. Labbé

CENTRE DE RECHERCHES POUR LA DÉFENSE
DEFENCE RESEARCH ESTABLISHMENT
VALCARTIER
Tel: (418) 844-4271

Québec, Canada May/mai 1984

ABSTRACT

This document describes two procedures for designing recursive digital filters from continuous-time filters when the ratio of the sampling frequency to the pole frequency is small. The coefficients of the proposed digital filters, which are derived from the step and ramp invariance of the corresponding analog filters, have been determined for real and complex poles. For higher-order filters realized in a parallel form, it is demonstrated that the discrete-time transfer function of digital filters obtained by the step and ramp invariance can be derived directly from the standard z-transformation or from the partial fraction expansion of the continuous-time transfer function. The discrete-time transfer functions of the step- and ramp-invariant filters realized in a cascade form have also been derived. Finally, the performance of these methods is demonstrated by plotting the magnitude and phase responses of the first- and second-order digital filters. For high-order Butterworth and elliptic filters, the magnitude responses of step-invariant and ramp-invariant filters are compared with those obtained by usual methods such as the standard z and the bilinear transformations.

RÉSUMÉ

Ce document décrit deux méthodes pour concevoir des filtres numériques récursifs à partir des filtres analogiques lorsque le rapport entre le taux d'échantillonnage et la fréquence du pôle est faible. Les coefficients des filtres numériques proposés, qui proviennent de l'invariance à l'échelon et à la rampe des filtres analogiques correspondants, ont été déterminés pour les pôles réels et complexes. Pour les filtres d'ordres plus élevés réalisés dans un réseau parallèle, il est démontré que la fonction de transfert en z des filtres numériques caractérisés par l'invariance à l'échelon et à la rampe peut être déduite directement de la transformée en z ou de la décomposition en fractions partielles de la fonction de transfert des filtres analogiques. On a aussi déduit la fonction de transfert en z des filtres invariants à l'échelon et à la rampe pour une réalisation dans un réseau en série. Finalement, la performance de ces méthodes est démontrée en traçant les réponses en amplitude et en phase des filtres numériques du premier et du deuxième ordre. Pour des filtres Butterworth et elliptiques d'ordres élevés, on compare la réponse en amplitude des filtres invariants à l'échelon et à la rampe avec celle obtenue par des méthodes courantes telles que la transformée en z et la transformée bilinéaire.

1.0 INTRODUCTION

As with analog filters, the approximation step in the design of digital filters is the process whereby a realizable transfer function that satisfies prescribed conditions is obtained. Several methods permit the derivation of recursive digital filters from the continuous-time transfer function of their analog counterpart when the ratio of the sampling frequency to the pole frequency (f_s/f_p) is sufficiently large. The methods constitute textbook material and include the impulse-invariant, matched z and bilinear transformations. On the other hand, they suffer from serious drawbacks such as aliasing and frequency warping, which lead to inappropriate approximations when f_s/f_p is small.

The two approximation methods described in this report, the step-invariant and ramp-invariant transformations, fill this gap by providing valid matches even when f_s/f_p is small. The proposed methods are an extension of the impulse-invariant transformation. With this technique, which is also called the standard z-transformation, the response of the derived digital filter to an impulse is identical to that of the sampled-impulse response of the continuous-time filter. In the step-invariant transformation, the response of analog filters is found by assuming that the input is approximated by a sequence of steps whose duration is set to the sampling period and whose amplitude corresponds to the instantaneous value of the input signal at the time of sampling. In the ramp-invariant transformation, the input signal consists of a sequence of ramps that join the sampled values. This procedure leads to the determination of the discrete-time transfer function of digital filters, whose response is identical to that of the reference analog filter in relation to the input signal (step or ramp).

In this report, discrete-time transfer functions were determined for first- and second-order filters with real and complex poles. Mappings from the continuous-time (Laplace transform) and discrete-time (z-transform) transfer functions were derived for the step- and ramp-invariant transformations. The methods were generalized for filters of any orders with poles of any multiplicity by considering partial fraction expansions in terms of first- and second-order transfer functions. This approach leads directly to a parallel implementation. The discrete-time transfer function of the step-invariant and ramp-invariant filters realized in a cascade form has also been derived.

This theoretical approach was validated by plotting the magnitude and phase response of first- and second-order digital filters derived by the step- and ramp-invariant transformations. These responses are compared with those of the analog filters and the impulse-invariant digital filters. Finally, for high-order Butterworth and elliptic filters, the magnitude responses of the step- and ramp-invariant filters are compared with those obtained by the impulse-invariant transformation, the bilinear transformation and the original analog filter.

This work was performed at DREV between September 1982 and February 1983 under PCN 21J05, Guidance and Control Concepts.

TABLE OF CONTENTS

2.0 BACKGROUND

Filtering is a process by which the frequency spectrum of a signal can be modified, reshaped, or manipulated according to some desired specification. It may imply amplifying or attenuating a range of frequency components, rejecting or isolating one specific frequency component, etc.

The digital filter is used to process discrete-time or sampled signals. It can be implemented by means of software or dedicated hardware, and it can be represented by a network comprising a collection of interconnected elements. The analysis of a digital filter determines the response of the filter network to a given excitation. Its design, on the other hand, consists in synthetizing and implementing a filter network so that a set of prescribed excitations results in a set of desired responses.

The design of a digital filter comprises at least two steps: the approximation and realization ones. The approximation step is the process of generating a transfer function satisfying a set of specifications that may concern the amplitude, phase, and possibly time-domain response of the filter. The realization step is the process of converting the transfer function into a filter network using interconnected unit delays, adders and multipliers.

In the approximation step, the wealth of knowledge acquired in the design of analog filters may be transposed to the design of their digital counterparts. The discrete-time transfer function (expressed in z-transform) is derived from the continuous-time transfer function (expressed in Laplace transform) of a reference analog filter of known characteristics. Several methods are currently available that perform such approximations: the invariant-impulse, matched z- and bilinear transformations.

Once the discrete-time transfer function of the digital filter has been obtained, this transfer function can be converted into a filter network. The realization of this filter network will not necessarily operate exactly as prescribed because the previous operations were carried out assuming that the components to be used are of infinite precision. These effects need to be studied and corrected as necessary. The realization step of the digital filter is fully described in many textbooks such as Refs. 1 and 2. The transfer function can be broken down into simpler transfer functions and be realized directly. However, if the transfer function is given as a sum of partial fractions or as a product of first- and second-order factors, it can be realized either in parallel or cascade form without any further modifications.

2.1 Impulse-Invariant Transformation

The impulse-invariant transformation (Refs. 1 to 5) yields a digital filter with an impulse response equal to the sampled impulse response of the continous filter. In this transformation, the input signal x(t) is sampled at frequency f_s. The response of the analog filter is found by assuming that it is excited by a sequence of impulses equally spaced at intervals T (the sampling period). The amplitude of impulses is equal to that of the sampled values of x(t).

Given that the analog filter has only simple poles, its transfer function is written as:

$$H_A(s) = A_0 + \sum_{i=1}^{N} \frac{A_i}{s + p_i} + \sum_{i=1}^{N1} \left\{ \frac{C_i}{s + d_i} + \frac{C_i^*}{s + d_i^*} \right\} \qquad [1]$$

The details of the derivation of this equation can be found in Appendix A.

The impulse-invariant transformation I(z) of eq. 1 gives

$$I(z) = A_0 + \sum_{i=1}^{N} \frac{A_i T}{1 - e^{-p_i T} z^{-1}} + \sum_{i=1}^{N1} \frac{A_{0i} + A_{1i} z^{-1}}{1 - (2e^{-\alpha_i T} \cos \beta_i T) z^{-1} + e^{-2\alpha_i T} z^{-2}} \quad [2]$$

where $z = e^{Ts}$, T being the sampling period

$$A_{0i} = T K_{1i}$$

$$A_{1i} = T e^{-\alpha_i T} [K_{1i} \cos \beta_i T + K_{2i} \sin \beta_i T]$$

$$K_{1i} = C_i^* + C_i = 2 \, \mathrm{Re}(C_i)$$

$$K_{2i} = (C_i^* - C_i) j = 2 \, \mathrm{Im}(C_i)$$

$$d_i = \alpha_i - j\beta_i$$

d_i^* = conjugate of d_i

The mapping relation between the s plane and the z plane can be deduced directly from eq. 2. It is written as

$$\frac{1}{s + p_i} \rightarrow \frac{T}{1 - z^{-1} e^{-p_i T}} \quad [3]$$

This method yields valid matches with the corresponding analog system only at high sampling rates and it is satisfactory only when the analog system is sufficiently band limited.

2.2 Matched z-Transformation

The matched z-transformation is a technique based on mapping the poles and zeros of the continuous-time filter. It is performed on the cascade form of the transfer function of analog filters. As shown in Appendix A, this form is written as

$$H(s) = K_s \frac{\prod_{i=1}^{M'} (s + m_i)}{\prod_{i=1}^{N'} (s + p_i)} \qquad [4]$$

The discrete-time transfer function of eq. 4 is given in Ref. 5 as

$$H(z) = (z + 1)^L K_s \frac{\prod_{i=1}^{M'} (z - e^{-m_i T})}{\prod_{i=1}^{N'} (z - e^{-p_i T})} \qquad [5]$$

where L is an integer whose value is equal to the number of zeros of H(s) at $s = \infty$. In this transformation, the poles of digital filters are identical to those obtained by the impulse-invariant transformation. However, the zeros do not correspond. In general, the use of the impulse-invariant or bilinear transformation is preferable to that of the matched z-transformation (Ref. 1).

2.3 Bilinear Transformation

A bilinear transformation is obtained by substituting s in the continuous-time transfer function H(s) by

$$s \rightarrow \frac{2}{T} \frac{1 - z^{-1}}{1 + z^{-1}} \qquad [6]$$

This transformation, which is used to circumvent the aliasing problem of the standard z-transformation, results in a nonlinear warping

of the frequency scale between the continuous-time frequency and the discrete-time one, according to the relation

$$\frac{\omega_A T}{2} = \tan \frac{\omega_D T}{2} \qquad [7]$$

where ω_A is the continuous-time frequency variable and ω_D is the discrete-time one.

3.0 STEP-INVARIANT TRANSFORMATION

The step-invariant transformation is an extension of the impulse-invariant technique. The response of the analog system is found by assuming that the input x(t) is approximated by a sequence of steps. The amplitude of steps corresponds to the instantaneous value of x(t) at the time of sampling and their duration is equal to sampling period T. In this case, the input signal is written as

$$x(t) = \sum_{n=0}^{\infty} X(nT) \{\mu(t - nT) - \mu(t - (n + 1) T)\} \qquad [8]$$

where $\mu(t - nT) = 0$ if $t < nT$ and
$= 1$ if $t > nT$.

In the following sections, an invariant-step transformation will be derived for first-order (real poles) and second-order (complex poles) terms of the partial fraction expansion given by eq. 1.

3.1 First-Order Terms (Real Poles)

Consider a real-partial fraction of the expansion given by eq. 1

$$\frac{Y(s)}{X(s)} = \frac{A}{s + p} \qquad [9]$$

We can derive from eq. 9 a difference equation that will give $y[(n + 1)T]$, the value of $y(t)$ at time t_{n+1}, and from $x(nT)$ and $y(nT)$, the values of $x(t)$ and $y(t)$ at time t_n. The transfer function must be rewritten by setting the initial condition of the output variable at time t_n. Then, the filter is stimulated by a pulse whose amplitude and duration are set to the instantaneous value of the input signal at time t_n and to the sampling period respectively. Substituting the input variable by the Laplace transformation of a pulse function of amplitude $x(nT)$ and multiplying this result with the transfer function of the filter yields a new relationship. Finding its inverse Laplace transformation and substituting t by (n+1)T gives the value of the output at time t_{n+1}.

If we take into account the initial condition of the variable $y(t)$ at time $t_n(=nT)$, noted by $y(nT)\ \delta(t - nT)$ where

$$\delta(t - nT) = 1 \text{ if } t = nT$$
$$= 0 \text{ elsewhere}$$

Thus, the transfer function of eq. 9 is transformed as

$$Y(s) = \frac{AX(s)}{s + p} + \frac{y(nT)\ e^{-nTs}}{s + p} \qquad [10]$$

Since the input variable at time t_n is a pulse of amplitude $x(nT)$, its Laplace transformation is

$$X(s) = \frac{x(nT)}{s} (e^{-nTs} - e^{-(n + 1)Ts}) \qquad [11]$$

Substituting eq. 11 in eq. 10 and finding the inverse Laplace transformation of this relation yields the following time function:

$$y(t) = \left\{\frac{Ax(nT)}{p}(1 - e^{-p(t - nT)}) + y(nT)\, e^{-p(t - nT)}\right\} \mu(t - nT)$$

$$- \frac{Ax(nT)}{p} (1 - e^{-p(t - (n + 1)T)}) \mu(t - (n + 1)T) \qquad [12]$$

Finally, let us determine the value of y(t) at time t_{n+1} by replacing t by (n + 1)T in eq. 12. This leads to

$$y[(n + 1)T] = \frac{Ax(nT)}{p} (1 - e^{-pT}) + y(nT)e^{-pT} \qquad [13]$$

Equation 13 is a finite difference equation whose discrete-time transfer function is

$$S(z) = \frac{Y(z)}{X(z)} = \frac{(A/p)\ (1 - e^{-pT})z^{-1}}{1 - e^{-pT}z^{-1}} \qquad [14]$$

By comparing eqs. 14 and 9, it is seen that the discrete-time transfer function can be obtained from the continuous-time transfer function by using the mapping relation

$$\frac{1}{s + p} \rightarrow \frac{(1/p)\ (1 - e^{-pT})z^{-1}}{1 - e^{-pT}z^{-1}} \qquad [15]$$

3.2 Second-Order Terms (Complex Poles)

Now consider one complex-partial fraction of the expansion given by eq. 1

$$\frac{C}{s + d} + \frac{C^*}{s + d^*} \qquad [16]$$

If we apply the substitution of eq. 15 to each of the individual terms of eq. 16, we find

$$\frac{\frac{C}{d}(1 - e^{-dT})z^{-1}}{1 - z^{-1}e^{-dT}} + \frac{\frac{C^*}{d^*}(1 - e^{-d^*T})z^{-1}}{1 - z^{-1}e^{-d^*T}} =$$

$$\frac{K_A z^{-2} + K_B z^{-1}}{1 - (2e^{-\alpha T}\cos\beta T)z^{-1} + e^{-2\alpha T}z^{-2}} \qquad [17]$$

where $K_A = K_1 e^{-2\alpha T} - K_1 e^{-\alpha T}\cos\beta T - K_2 e^{-\alpha T}\sin\beta T$

$$K_B = K_1 - K_1 e^{-\alpha T}\cos\beta T + K_2 e^{-\alpha T}\sin\beta T$$

$$K_1 = (C/d) + (C^*/d^*)$$

$$K_2 = (C^*/d^* - C/d)j$$

The step-invariant transformation of analog filters described by eq. 1, whose N real poles and N1 complex poles are simple, is determined by substituting eqs. 15 and 17 in eq. 1. This gives

$$S(z) = A_0 + \sum_{i=1}^{N} \frac{\frac{A_i}{p_i}(1 - e^{-p_i T})z^{-1}}{1 - e^{-p_i T}z^{-1}}$$

$$+ \sum^{N1} \frac{K_{Ai}z^{-2} + K_{Bi}z^{-1}}{1 - (2e^{-\alpha_i T}\cos\beta_i T)z^{-1} + e^{-2\alpha_i T}z^{-2}} \qquad [18]$$

4.0 RAMP-INVARIANT TRANSFORMATION

The z-transform of this technique can be derived from the Laplace transform by applying the same operations that yield the z-transformation of the step invariance, the only difference being that the analog filter at time t_n is excited by a ramp such as:

$$x(t_n) = \{x[(n-1)T] + \frac{x(nT) - x[(n-1)T]}{T}\} \{\mu[t - (n-1)T] - \mu(t - nT)\} \quad [19]$$

If we apply the following procedure to a real-partial fraction (eq. 9) of the expansion given by eq. 1:

1) Transformation of eq. 9 to eq. 10: this operation allows us to consider initial conditions of the output variable at time t_n.

2) Substitution of X(s) in eq. 10 by

$$\{\frac{x[(n-1)T]}{s} + \frac{x(nT) - x[(n-1)T]}{Ts^2}\} (e^{-(n-1)Ts} - e^{-nTs}) \quad [20]$$

which is the Laplace transformation of the ramp function (eq. 19) at time t_n.

3) Solve eq. 10 to derive a relation as a function of time and replace t by nT to get the value of the output at time t_n.

A difference equation that gives y(nT) from x(nT), x[(n-1)T] and y [(n-1)T] can be derived. Its z-transformation is

$$\frac{Y(z)}{X(z)} = \frac{A\{\frac{1}{p}(1 - e^{-pT}z^{-1}) - \frac{1}{p^2T}(1 - e^{-pT})(1 - z^{-1})\}}{1 - e^{-pT}z^{-1}} \qquad [21]$$

In comparing eqs. 21 and 9, we deduce that the ramp invariance can be obtained from H(s) by using the mapping relation

$$\frac{1}{s + p} \rightarrow \frac{\frac{1}{p}(1 - e^{-pT}z^{-1}) - \frac{1}{p^2T}(1 - e^{-pT})(1 - z^{-1})}{1 - e^{-pT}z^{-1}} \qquad [22]$$

For complex poles, we substitute the mapping relation of eq. 22 in each term of eq. 16 to find:

$$\frac{K_C + K_D z^{-1} + K_E z^{-2}}{1 - (2e^{-\alpha T}\cos \beta T)z^{-1} + e^{-2\alpha T}z^{-2}} \qquad [23]$$

where $K_1 = (C/d) + (C^*/d^*)$

$$K_3 = [C/d^2 + (C/d^2)^*]/T$$

$$K_4 = [(\frac{C}{d^2})^* - \frac{C}{d^2}]\frac{1}{T}$$

$$K_5 = -e^{-\alpha T}(K_3 \cos \beta T + K_4 \sin \beta T)$$

$$K_C = K_1 - K_3(1 - 2e^{-\alpha T}\cos \beta T) + K_5$$

$$K_D = K_3(1 - 2e^{-\alpha T}\cos \beta T - e^{-2\alpha T}) - K_1(2e^{-\alpha T}\cos \beta T) - 2K_5$$

$$K_E = e^{-2\alpha T}(K_1 + K_3) + K_5$$

For simple poles, the ramp-invariant transformation of analog filters characterized by N real poles and Ni complex poles gives:

$$R(z) = A_0 + \sum_{i=1}^{N} \frac{A_i}{p_i} \frac{(1 - \frac{1 - e^{-p_i T}}{p_i T}) + (\frac{1 - e^{-p_i T}}{p_i T} - e^{-p_i T})z^{-1}}{1 - e^{-p_i T} z^{-1}}$$

$$+ \sum_{i=1}^{Ni} \frac{K_{Ci} + K_{Di} z^{-1} + K_{Ei} z^{-2}}{1 - (2e^{-\alpha_i T} \cos \beta_i T)z^{-1} + e^{-2\alpha_i T} z^{-2}} \qquad [24]$$

5.0 GENERALIZED s-z TRANSFORMATION

In this chapter, we will first establish a procedure that derives the step- and ramp-invariant transformations directly from the impulse-invariant transformation. Then, this procedure will be used to determine the step and ramp invariances of analog filters containing multiple poles.

The mapping relation between the s and z planes that gives the step invariance is from eq. 15

$$\frac{1}{s + p} \rightarrow \frac{(1/p)(1 - e^{-pT})z^{-1}}{1 - e^{-pT} z^{-1}}$$

This relation can be rewritten as

$$\frac{1}{s + p} \rightarrow (1 - z^{-1})(\frac{1/p}{1 - z^{-1}} - \frac{1/p}{1 - e^{-pT} z^{-1}}) = (1 - z^{-1}) Z(\frac{1}{s(s + p)})$$

where Z is defined as the operator corresponding to the invariant-impulse response of analog systems or standard z-transformation. Also, the mapping relation of the ramp invariance (eq. 22) can be expressed as

$$\frac{1}{s+p} \cdot \frac{1}{p} = \frac{(1 - e^{-pT} z^{-1})/p^2}{1 - e^{-pT} z^{-1}}$$

$$= \frac{(1 - z^{-1})^2}{Tz^{-1}} \left\{ \frac{T z^{-1}/p}{(1 - z^{-1})^2} - \frac{(1 - e^{-pT}) z^{-1}/p^2}{(1 - z^{-1})(1 - e^{-pT} z^{-1})} \right\} =$$

$$\frac{(1 - z^{-1})^2}{Tz^{-1}} \left[z\left\{ \frac{1}{s^2 (s + p)} \right\} \right] \qquad [25]$$

Thus, it is shown that the step and ramp invariances can be derived from the impulse invariance. This operation consists in multiplying the transfer function of an analog filter H(s) by the Laplace transformation of the unit-step function (1/s) or the unit-ramp function ($1/s^2$), finding the standard z-transformation of this relation and, finally, dividing the result by the standard z-transformation of the unit-step function which is $1/(1 - z^{-1})$ or the unit-ramp function, which is $T z^{-1}/(1 - z^{-1})^2$.

The invariant-step response S(z) and the invariant-ramp response R(z) of an analog system whose transfer function is H(s) can then be put in the form

$$S(z) = \left[z\left\{ \frac{H(s)}{s} \right\} \right] (1 - z^{-1}) \qquad [26]$$

$$\text{and } R(z) = \left[z\left\{ \frac{H(s)}{s^2} \right\} \right] \frac{(1 - z^{-1})^2}{Tz^{-1}} \qquad [27]$$

This procedure allows the determination of the step and ramp invariances of analog filters whose transfer function contains multiple poles. In Appendix A, this transfer function is expressed as:

$$H(s) = A_0 + \sum_{i=1}^{N} \sum_{k=1}^{M_i} \frac{A_{ik}}{(s + p_i)^k} + \sum_{i=1}^{N1} \sum_{k=1}^{M1_i} \frac{C_{ik}}{(s + d_i)^k} + \frac{C_{ik}^*}{(s + d_i^*)^k} \qquad [28]$$

where M_i and $M1_i$ in the double summation indicates the multiplicity of the real and complex poles.

The standard z-transform of these functions is given in Ref. 6 as:

$$\frac{1}{(s + p_i)^{\ell + 1}} = \frac{T^\ell e^{-\ell p_i T} D_\ell(a_i) z^{-\ell}}{(1 - e^{-p_i T} z^{-1})^{\ell + 1}} \qquad [29]$$

where $D_\ell(a_i)$ is defined by

$$D_\ell(a_i) = \begin{vmatrix} 1 & 1 - \frac{z}{a_i} & 0 & \cdots & 0 \\ \frac{1}{2!} & 1 & 1 - \frac{z}{a_i} & \cdots & 0 \\ \frac{1}{3!} & \frac{1}{2!} & 1 & \cdots & 0 \\ \cdots & \cdots & \cdots & & \cdots \\ \frac{1}{\ell!} & \frac{1}{(\ell - 1)!} & \frac{1}{(\ell - 2)!} & \cdots & 1 \end{vmatrix}$$

where $a_i = e^{-p_i T}$ and $D_0(a_i) \triangleq 1$. For complex poles, p_i and a_i are replaced by d_i and b_i respectively ($b_i = e^{-d_i T}$).

The derivation of the step invariance can be found by substituting eq. 28 in eq. 26. This yields

$$S(z) = A_0 + \{\sum_{i=1}^{N}\sum_{k=1}^{M_i}\frac{A_{ik}}{p_i^k} - (1-z^{-1})\sum_{\ell=0}^{k-1}\frac{A_{ik}\,T^\ell\,a_i^\ell\,D_\ell(a_i)z^{-\ell}}{p_i^{k-\ell}\,(1-a_iz^{-1})^{\ell+1}}\}$$

$$+\{\sum_{i=1}^{N1}\sum_{k=1}^{M1_i}\frac{C_{ik}}{d_i^k}+\frac{C^*_{ik}}{d_i^{*k}} - (1-z^{-1})\sum_{\ell=0}^{k-1}T^\ell z^{-\ell}\,[\frac{C_{ik}\,b_i^\ell\,D_\ell(b_i)}{d_i^{k-\ell}\,(1-b_iz^{-1})^{\ell+1}}$$

$$+\frac{C^*_{ik}\,b_i^{*\ell}\,D_\ell(b_i^*)}{d_i^{*k-\ell}\,(1-b_i^*z^{-1})^{\ell+1}}]\}$$

[30]

The derivation of the ramp invariance consists in substituting eq. 28 in eq. 17. This leads to

$$R(z) = A_0 + \{\sum_{i=1}^{N}\sum_{k=1}^{M_i}\frac{A_{ik}}{p_i^k} - \frac{A_{ik}\,k(1-z^{-1})}{p_i^{k+1}\,T\,z^{-1}}$$

$$+\frac{(1-z^{-1})^2}{T\,z^{-1}}\sum_{\ell=0}^{k-1}\frac{A_{ik}(k-\ell)\,T^\ell\,a_i^\ell\,D_\ell(a_i)z^{-\ell}}{p_i^{k+1-\ell}\,(1-a_iz^{-1})^{\ell+1}}\}$$

$$+\{\sum_{i=1}^{N1}\sum_{k=1}^{M1_i}\frac{C_{ik}}{d_i^k}+\frac{C^*_{ik}}{d_i^{*k}} - [\frac{C_{ik}}{d_i^{k+1}}+\frac{C^*_{ik}}{d_i^{*k+1}}]\,\frac{k\,(1-z^{-1})}{T\,z^{-1}}$$

$$+\frac{(1-z^{-1})^2}{T\,z^{-1}}\sum_{\ell=0}^{k-1}(k-\ell)\,T^\ell z^{-\ell}\,[\frac{C_{ik}\,b_i^\ell\,D_\ell(b_i)}{d_i^{k+1-\ell}\,(1-b_iz^{-1})^{\ell+1}}$$

$$+\frac{C^*_{ik}\,b_i^{*\ell}\,D_\ell(b_i^*)}{d_i^{*k+1-\ell}\,(1-b_i^*z^{-1})^{\ell+1}}]\}$$

[31]

Chapters 3.0 to 5.0 derived the step- and ramp-invariant digital filters from the partial fraction expansion of the continuous-time transfer functions. This design procedure leads directly to a realization in a parallel form. If the cascade or direct form is desired, it can be obtained by substituting the mapping relations of eqs. 15 and 22 into the transfer function of analog filters expressed as a cascade form of first- and second-order blocks. The results are presented in Appendix B.

6.0 COMPARISON OF THE METHODS

The invariant-impulse, matched z- and bilinear transformations or either of the two methods developed in this report lead to different discrete-time transfer functions and, in some cases, to different realizations. At sufficiently high f_s/f_p, their time, gain and phase responses are nearly the same, and the step- and ramp-invariant transformations will be unnecessarily sophisticated. In this chapter, it will be shown that, at low values of f_s/f_p, the sophistication inherent in these meth- ods is necessary for transposing the characteristics of analog filters in the discrete-time domain.

First, the approximation of the first- and second-order digital filters with the impulse-, step- and ramp-invariant transformations have been considered. The frequency responses in magnitude and in phase of the transfer functions of the filters obtained by each method have been produced for the second-order band-pass filter, the first- and second-order low-pass filters and the first- and second-order high-pass filters. The frequency responses of the analog filters are given as a reference while those of the digital filters are given for a set of three values of f_s/f_p: 100, 10 and 4. In all cases, the pole frequency f_p and the gain of the analog filter at f_p were set to 1 kHz and 0 dB respectively.

The exercise was repeated for higher-order filters such as the Butterworth and elliptic low-pass, high-pass, band-pass and band-reject filters. In this case, only the frequency responses in magnitude were produced. However, the impulse-invariant, bilinear, step-invariant and ramp-invariant transformations were compared.

6.1 Comparison of the Methods for Deriving First- and Second-Order Filters

This comparison shows the differences between these types of digital filters in the time, magnitude and phase responses when small f_s/f_p ratios are used. It leads to the determination of the best procedure for designing high-order filters since they are merely a combination of first- and second-order terms.

First, let us consider a second-order band-pass filter with the following specifications: quality factor Q = 10, resonant frequency f_o = 1 kHz and gain at resonant frequency = 1. This is the special case of eq. A.5 where

$$H(s) = \frac{(\omega_o/Q)s}{s^2 + (\omega_o/Q)s + \omega_o^2}$$

Figure 1 shows the performances of the three types of digital filters for various sampling frequencies (f_s = 20 f_o, 10 f_o, 4 f_o and 2.5 f_o) when the input is excited by a step function of amplitude equal to 1. Each time the ratio f_s/f_p is changed, the coefficients of the filters are recalculated to maintain the resonant frequency constant. From Fig. 1, we deduce that the step- and ramp-invariant procedures simulate exactly the time response of the continuous filter. The impulse-invariant method generates an offset at the output of the filter that increases when the sampling frequency decreases.

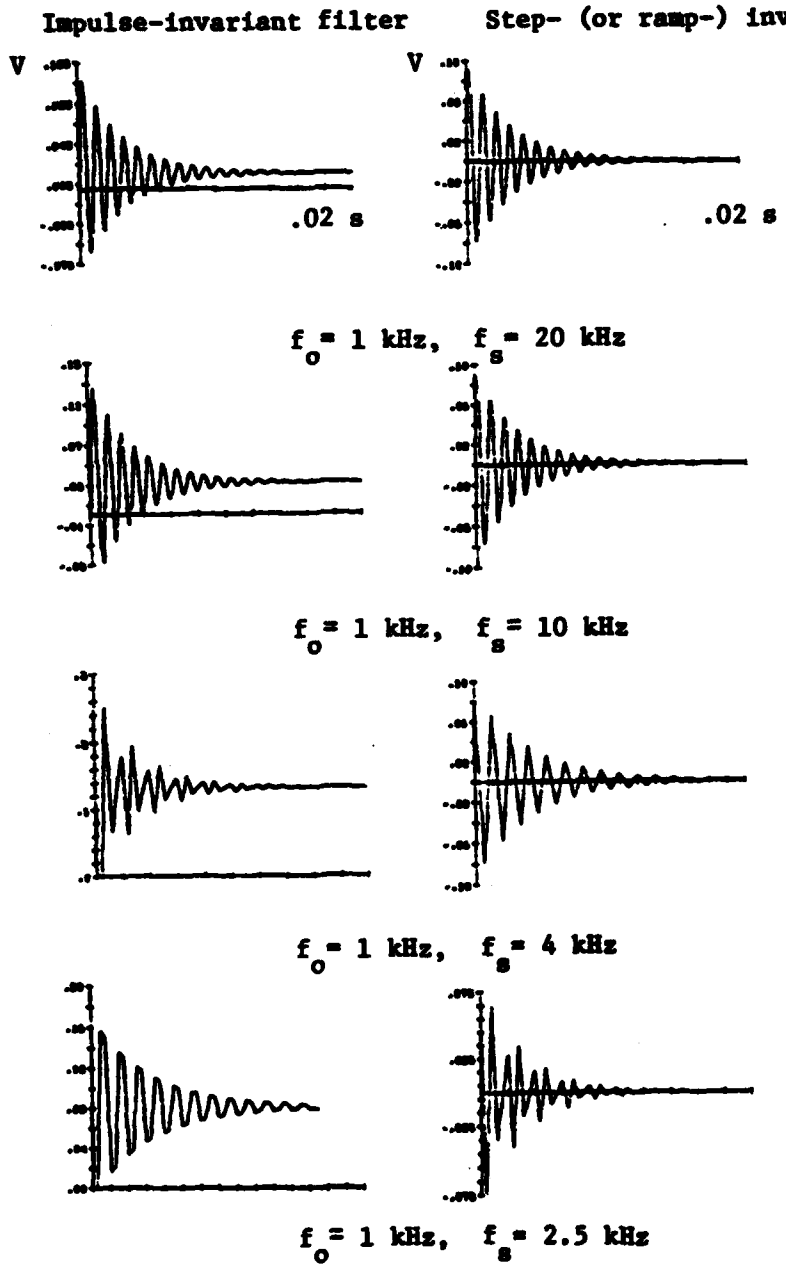

FIGURE 1 - Comparison between the step- (or ramp-) invariant method and the impulse-invariant method in the time response to a step-function input of a second-order band-pass filter

The behaviour of the time response is explained by examining the magnitude and phase responses of the three digital filters plotted in Fig. 2 for a set of three sampling frequencies (f_s = 100, 10 and 4 f_o). The responses of the corresponding analog filters are also plotted in this figure. This provides a reference for determining the performance of the digital filters. The ramp-invariant method produces a digital filter with a frequency response in amplitude and in phase that corresponds to the response of the continuous filter for a frequency band of 0 to $f_s/2$. In this region, its frequency response does not depend on the sampling frequency. The step-invariant filter has a magnitude response similar to that of the ramp-invariant filter. However, its phase response does not match the desired response around the resonant frequency. The difference between the analog and digital responses does not exceed 30° as the sampling frequency is set to 4 f_o. The response of the impulse-invariant filter is identical to that of the analog filter only in the frequency band located around the resonant frequency. Depending on the sampling frequency, the attenuation of the filter in the frequency band smaller than f_o becomes limited to a fixed value rather than following the slope of 40 dB/decade. For example, at $f_o/10$, the digital filter gives an error in amplitude that varies from 12 to 18 dB as the sampling frequency falls between 10 f_o and 4 f_o. A difference between the digital filter and its analog counterpart is also obeserved in the phase response. It can attain 90° within the full bandwidth ($f_s/2$) when f_s is set to 4 f_o.

Legend for Figures 2 through 6

.....	Continuous-time filter
-·-·-·-·-·-	Digital filter when f_s = 100 kHz
— — — — —	Digital filter when f_s = 10 kHz
----------	Digital filter when f_s = 4 kHz

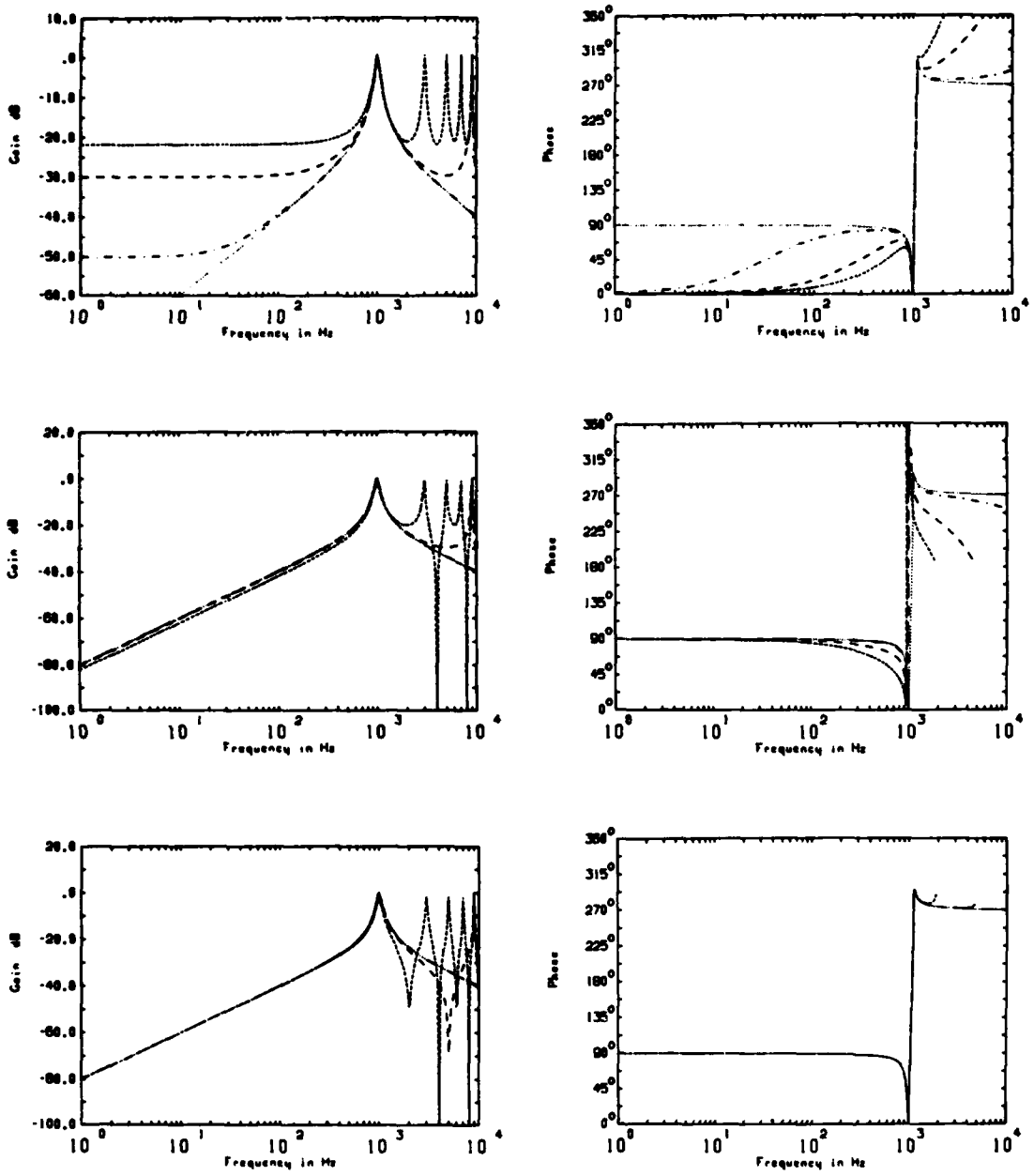

FIGURE 2 - Magnitude and phase responses of a second-order band-pass digital filter obtained by the impulse-invariant, step-invariant and ramp-invariant methods for various sampling frequencies

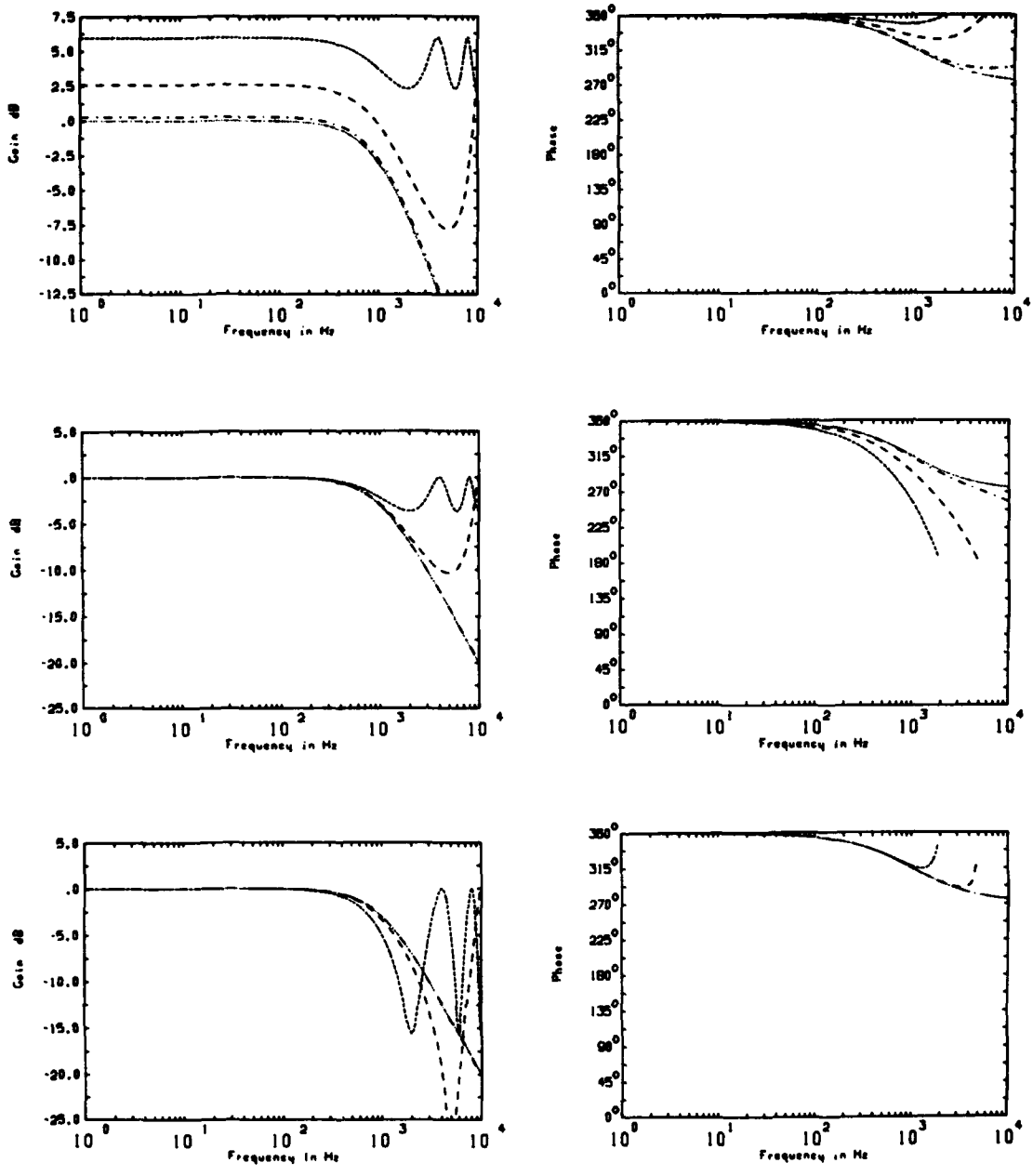

FIGURE 3 - Magnitude and phase responses of a first-order low-pass digital filter obtained by the impulse-, step- and ramp-invariant methods for various sampling frequencies

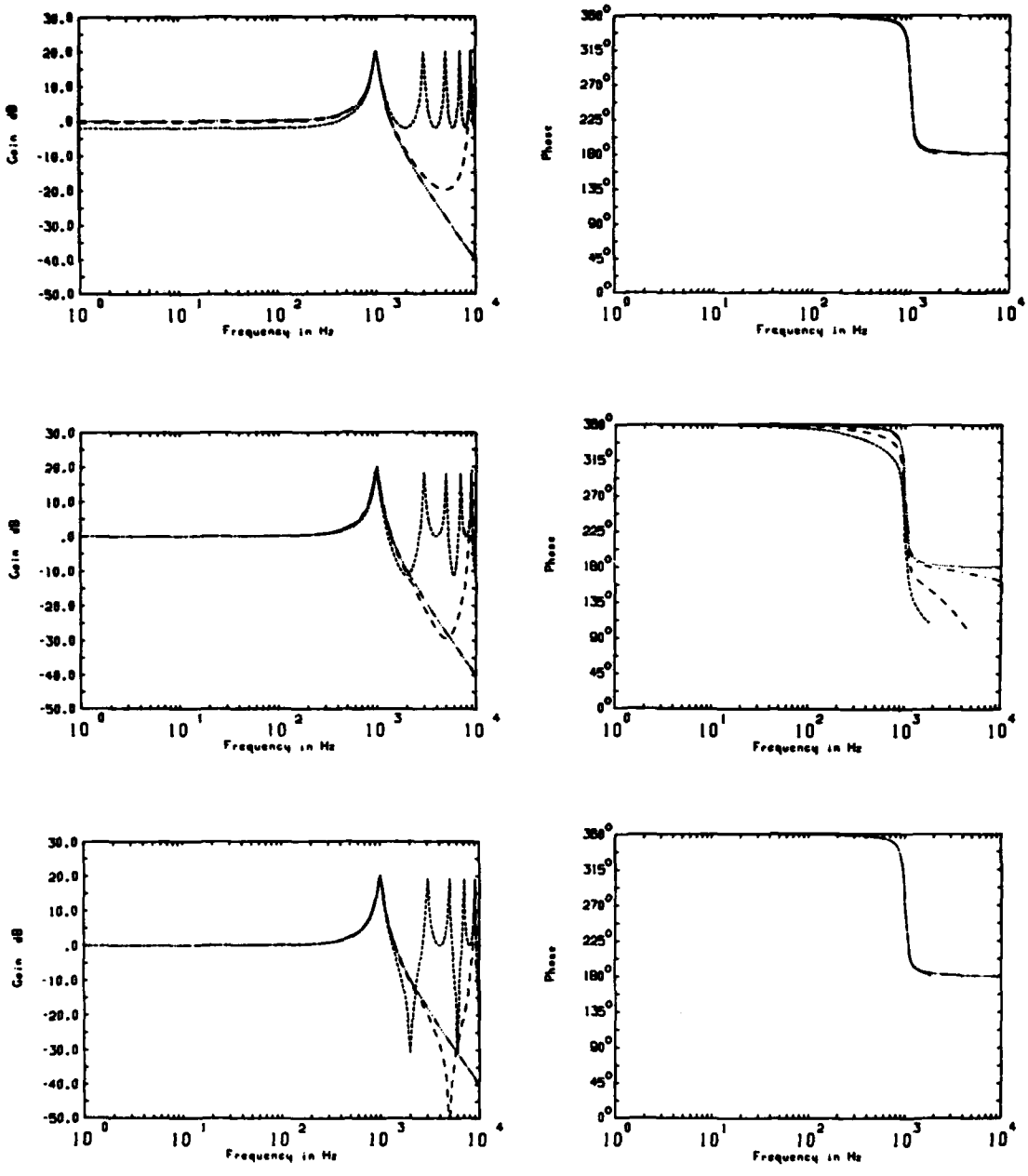

FIGURE 4 - Magnitude and phase responses of a second-order low-pass digital filter obtained by the impulse-, step- and ramp-invariant methods for various sampling frequencies

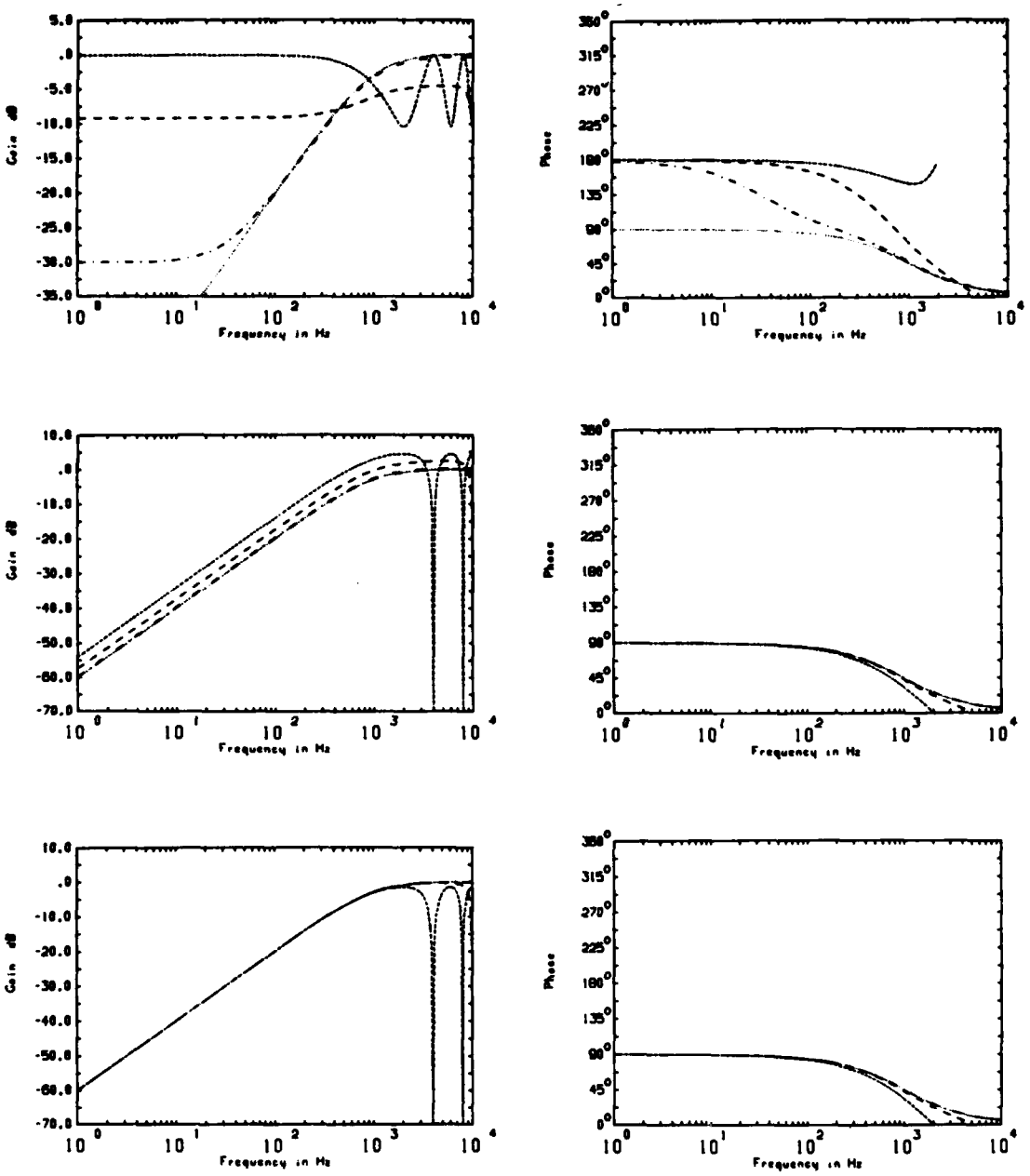

FIGURE 5 - Magnitude and phase responses of a first-order high-pass digital filter obtained by the impulse-, step- and ramp-invariant methods for various sampling frequencies

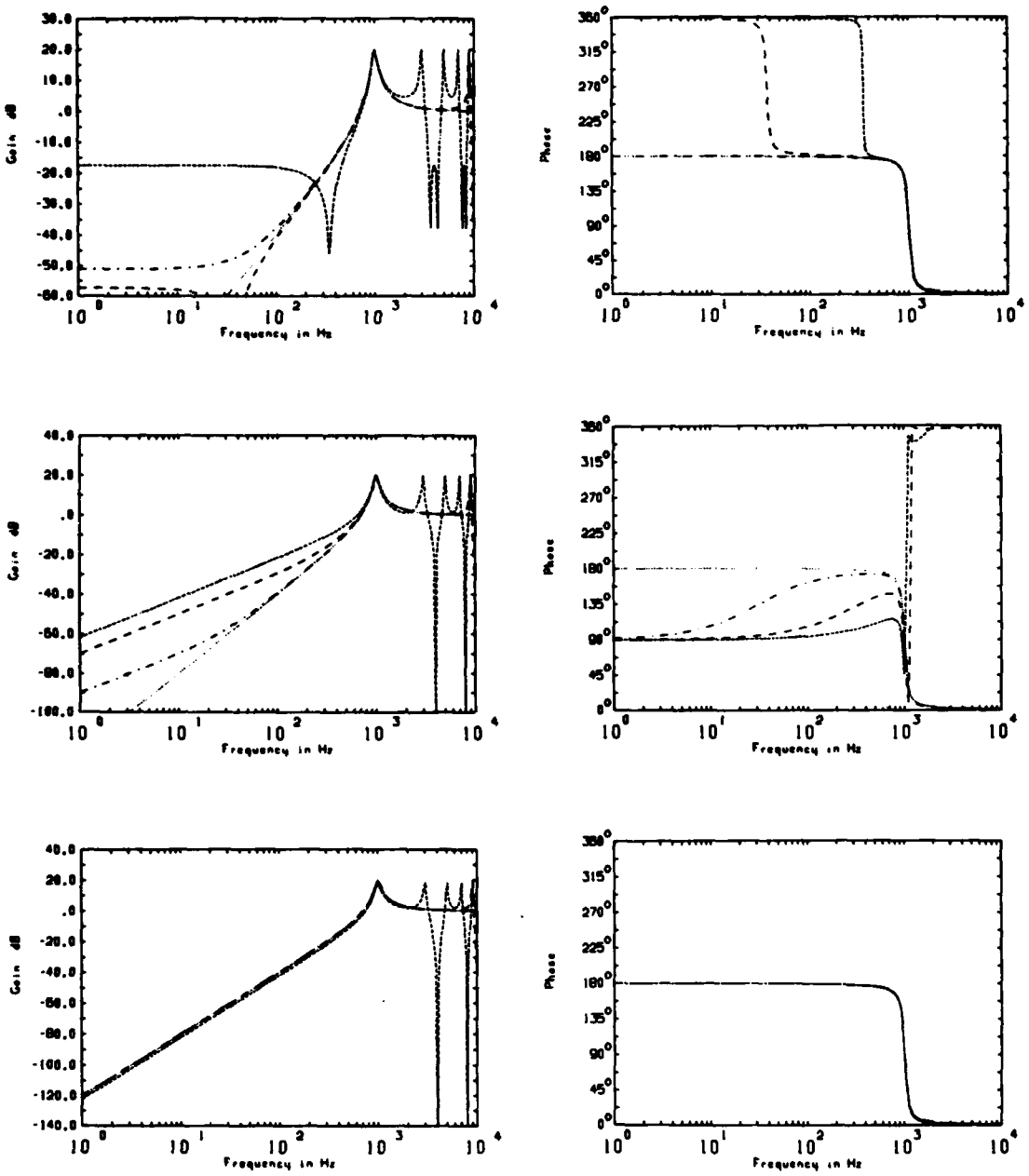

FIGURE 6 - Magnitude and phase responses of a second-order high-pass digital filter obtained by the impulse-, step- and ramp-invariant methods for various sampling frequencies

The discrepancies in the magnitude and phase responses also exist for the low- and high-pass filters. Figures 3 and 4 illustrate these responses of the first- and second-order low-pass filters for the step-, ramp- and impulse-invariant procedures when the sampling frequencies are set to 100, 10 and 4 f_p. The pole frequency and the gain of the filters are maintained constant at 1 kHz and 1 respectively. The quality factor Q of the second-order filters is set to 10. The impulse-invariant filter generates an error in magnitude that varies with the sampling rate. When f_s is set at 4 f_p, the error is limited to 6 dB for the first-order filter and to 3 dB for the second-order filter in the frequency band of 0 to $f_s/2$. On the other hand, the low-pass digital filters from the step-invariant and ramp-invariant methods simulate exactly the characteristics of their analog counterparts for a frequency band lower than $f_s/2$, except that the phase of the second-order step-invariant filter is slightly disturbed around the resonant frequency.

Finally, the magnitude and phase response of first- and second-order high-pass filters are illustrated in Figs. 5 and 6 for the same operating conditions as for the low-pass ones. For the first-order model, the preservation of the analog filter's characteristics by the impulse-invariant method requires a high sampling rate (> 100 f_p). For the second-order model, the analog filter's characteristics are preserved on a narrow frequency band. The attenuation of the amplitude becomes limited to a constant value in the frequency band lower than $f_s/2$ rather than following a constant slope of 40 dB/decade. The attenuation value and the starting frequency of this phenomenon vary with the sampling rate. The step invariance preserves the characteristics of the first-order high-pass filter within the frequency band of 0 to $f_s/2$ but, at small f_s/f_p ratios, a constant shift in the magnitude response is observed. This shift varies in function of the sampling rate and, for example, it is about 8 dB at $f_s = 4\ f_p$. In addition, an error in the phase response exists around the pole frequency. For the second-order filter, the constant amplitude attenuation encountered in the impulse-

invariant filter is replaced by an attenuation reduced to a slope of 20 dB/octave. The filter also generates a phase error of 90° in the useful frequency band for sampling rates smaller than 10 f_p. The magnitude and phase responses of the first- and second-order high-pass digital filters from the ramp invariance correspond to the responses of the high-pass analog filter, provided that the frequency band is limited to $f_s/2$.

Thus, step- and ramp-invariant filters give more accurate frequency response in magnitude and in phase than the impulse-invariant filter for all the cases of first- and second-order filters when small f_s/f_p ratios are used. In this condition, the impulse invariance can be performed only on the second-order low-pass filter. The step invariance gives accurate frequency responses for low-pass and band-pass filters with small phase errors around the complex poles. Finally, the ramp invariance produces a close match between the frequency responses of digital and analog filters.

6.2 Comparison of the Methods for Deriving Higher-Order Filters

The next set of figures (Figs. 7 to 15) shows the frequency magnitude characteristics of digital filters obtained by the step-, ramp- and impulse-invariant and the bilinear transformations of high-order Butterworth and elliptic filters. For further details about Butterworth and elliptic filter synthesis, see Ref. 7. In all examples, the response of digital filters is presented for various sampling frequencies (1000, 100, 10 and 4 kHz) and it is accompanied by the response of the corresponding analog filter. Figures 7 to 10 illustrate fifth-order low-pass and high-pass Butterworth and elliptic filters. The cut-off frequency and the gain of these filters are maintained at 1 kHz and 1 respectively. In addition, for the elliptic filters, the stop-band attenuation is at least 40 dB and the pass-band ripple is limited to 3 dB. The band-pass and band-reject Butterworth

and elliptic filters of Figs. 11 to 14 were derived from a transformation performed on the corresponding low-pass filters (Ref. 7). The lower- and upper-cutoff frequencies of these filters are located at 700 Hz and 1.4 kHz. The poles and zeros of these analog filters are given in Appendix C. The cutoff frequency of the high- and low-pass filters and the center frequency of the band-pass and band-reject ones are noted by f_p. In addition, the step and ramp invariances of analog filters presented in this group of figures were performed on the partial-fraction expansion which yielded a parallel realization.

This set of figures shows that the impulse-invariant transformation can be applied only to Butterworth low-pass and band-pass filters. In the first case, a close match between the analog and digital filter is obtained. In the second case, the magnitude response in the low-frequency band does not correspond to that of its analog counterpart when the ratio f_s/f_p becomes smaller than 10. In all the other examples, the impulse-invariant method is unacceptable. For elliptic low-pass and band-pass filters, the equiripple character of the stop-band response was destroyed by the aliasing effect. Finally, the aliasing renders this transformation entirely useless as a digital band-reject or high-pass filter (Butterworth or elliptic).

The bilinearly transformed filters are essentially identical to the original analog filter when the ratio f_s/f_p is greater than 10. However, the poles of the digital filters are moved in relation to the sampling frequency. This effect, called nonlinear frequency warping, is usually observed when the sampling frequency is smaller than 10 f_p. Thus, this method does not correctly preserve the magnitude response of analog filters at small values of f_s/f_p.

The step and ramp invariance of low-pass and band-pass filters produce digital filters whose magnitude response does not depend on the sampling frequency in the frequency band of 0 to $f_s/2$. For high-pass

and band-reject filters, the magnitude response of the step-invariant digital filters is unacceptable at small values of the ratio f_s/f_p. The ramp-invariant method can be used to digitize high-pass and band-reject filters but the magnitude responses of analog and digital systems are not identical when the ratio f_s/f_p becomes smaller than 10. In this case, the equiripple character of elliptic high-pass and band-reject filters is not correctly simulated. The magnitude response of the Butterworth high-pass filter in the low-frequency band is not preserved by the ramp-invariant filter. Moreover, the attenuation of the band-reject Butterworth filter in the stop-band region is limited to a value that varies as a function of the sampling frequency.

If the realization in cascade is used for the ramp invariance of high-pass and band-reject filters, better approximation of the analog filters is obtained. Figure 15 reveals that the digital Butterworth filters preserve the magnitude response of their analog counterparts. However, a small shift in the magnitude response of the digital high-pass filter can be observed when the ratio f_s/f_p becomes smaller than 10. For the elliptic high-pass and band-reject filters, a close match between analog and digital systems exists if the ratio f_s/f_p is maintained above 10. Cascade realization can also be performed on low-pass and band-pass step-invariant filters but the magnitude response of these filters is less accurate than that obtained by the ramp-invariant filters realized in a parallel form.

Legend for Figures 7 through 15

_____ Continuous-time filter

. . . . . Digital filter when f_s = 1000 kHz

– – – – – – – – – – – – Digital filter when f_s = 100 kHz

. . . . . Digital filter when f_s = 10 kHz

–·–·–·–·–·–·–·– Digital filter when f_s = 4 kHz

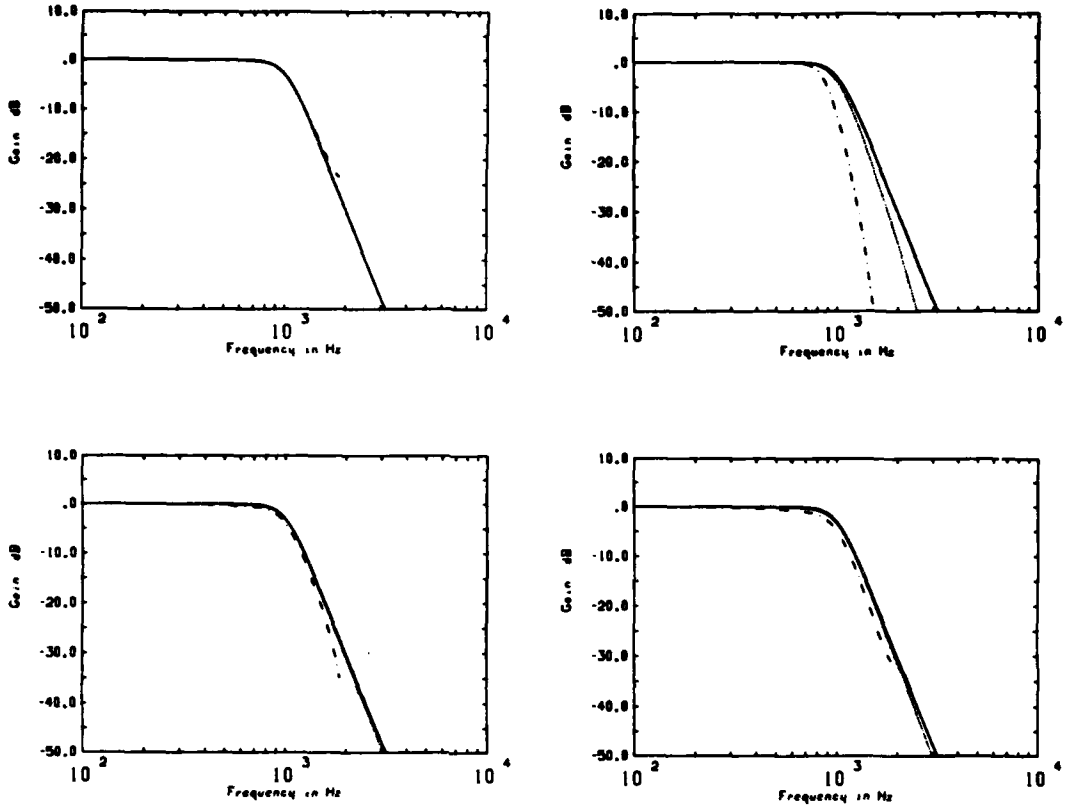

FIGURE 7 - Magnitude response of a Butterworth low-pass digital filter obtained by the impulse-invariant, the bilinear, the step- and the ramp-invariant transformations for various sampling frequencies

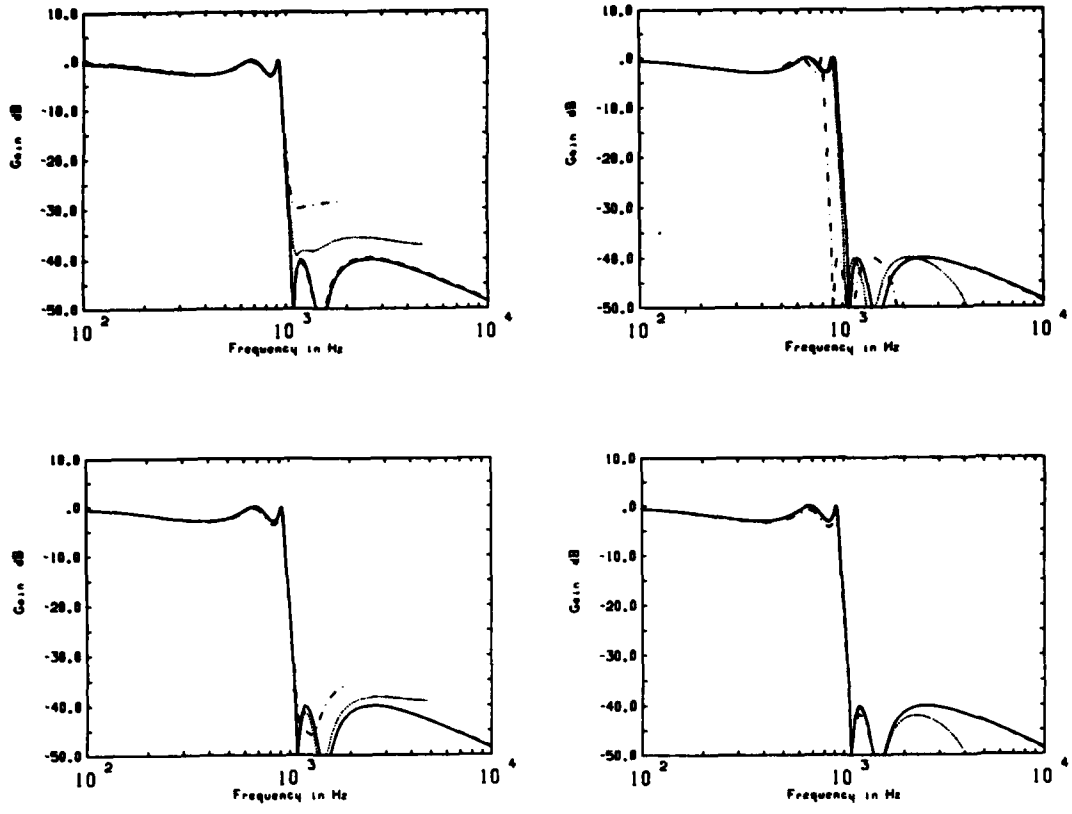

FIGURE 8 - Magnitude response of an elliptic low-pass digital filter obtained by the impulse-invariant, the bilinear, the step- and the ramp-invariant transformations for various sampling frequencies

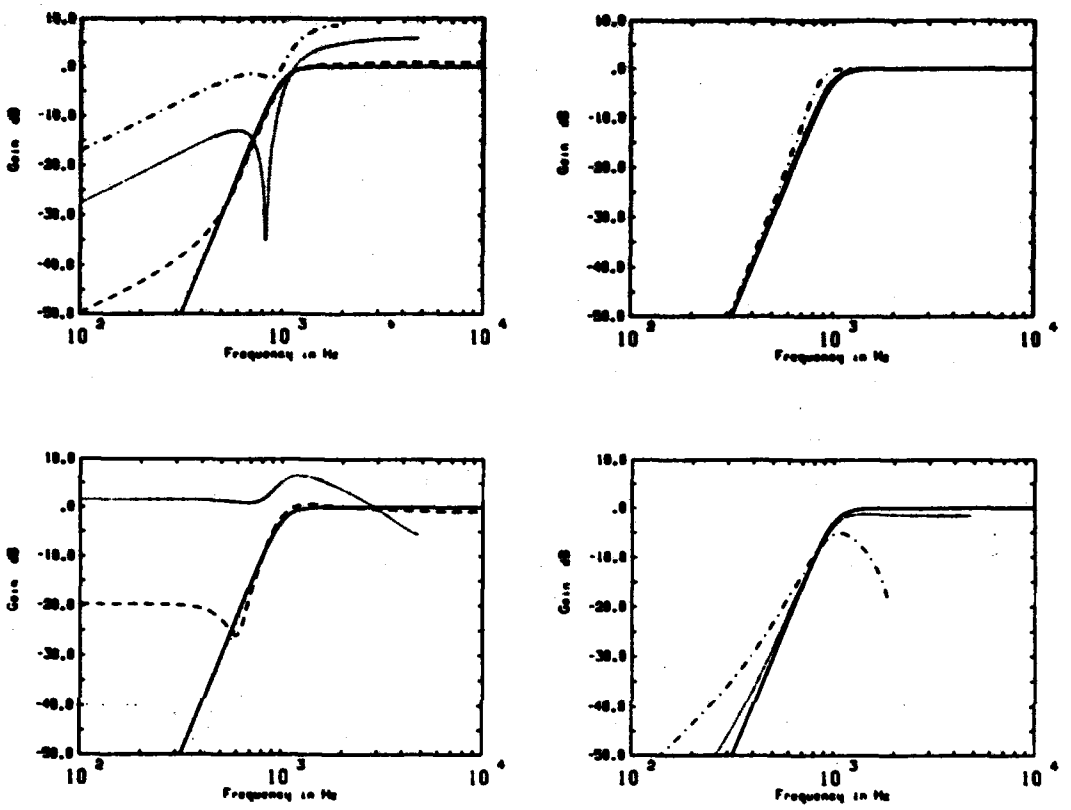

FIGURE 9 - Magnitude response of a Butterworth high-pass digital filter obtained by the impulse-invariant, the bilinear, the step- and the ramp-invariant transformations for various sampling frequencies

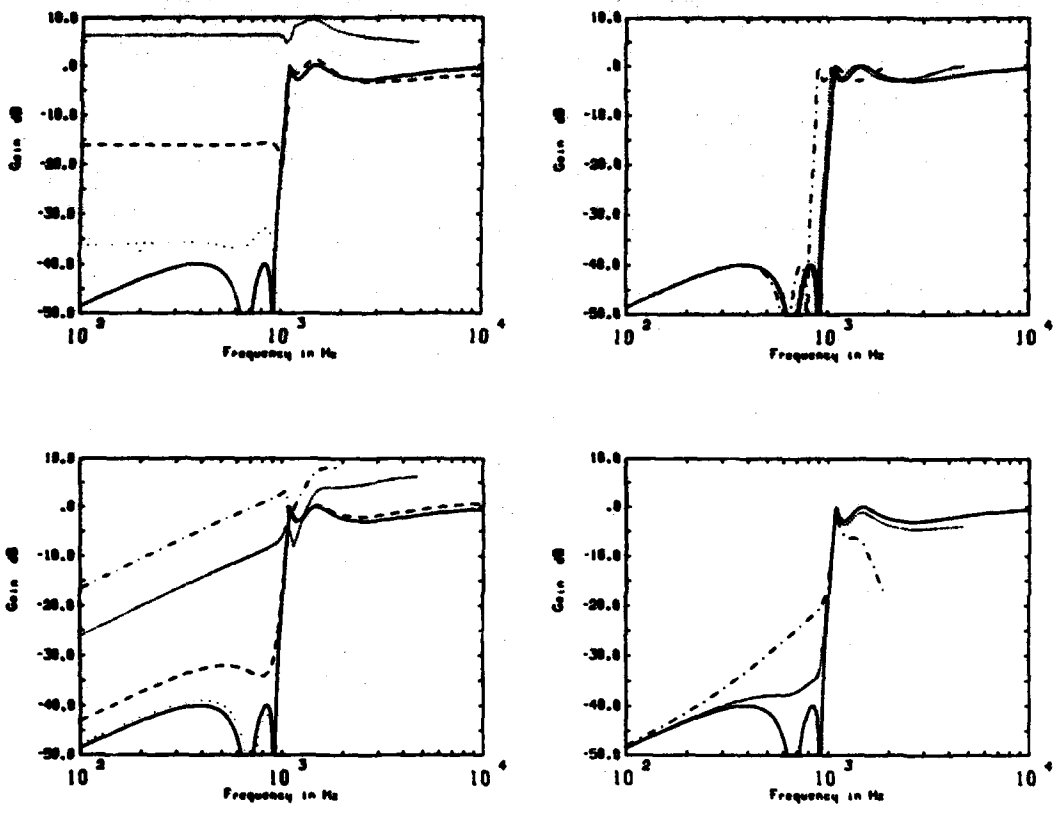

FIGURE 10 - Magnitude response of an elliptic high-pass digital filter obtained by the impulse-invariant, the bilinear, the step- and the ramp-invariant transformations for various sampling frequencies

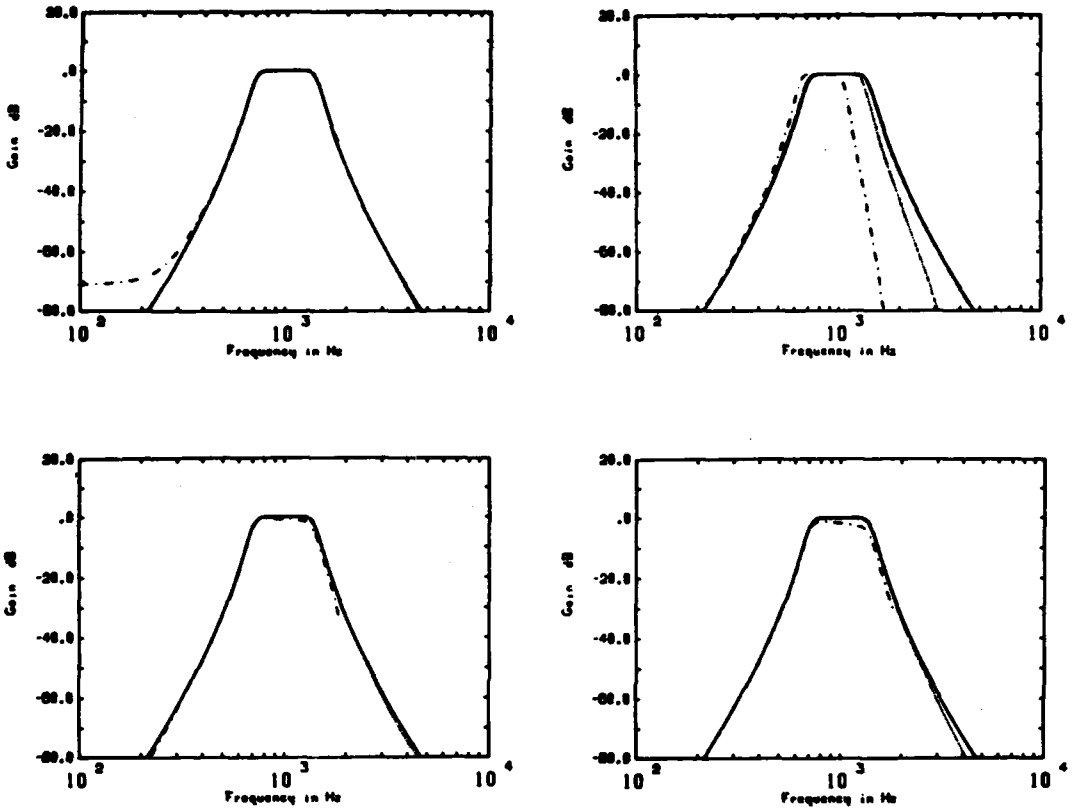

FIGURE 11 - Magnitude response of a Butterworth band-pass digital filter obtained by the impulse-invariant, the bilinear, the step- and the ramp-invariant transformations for various sampling frequencies

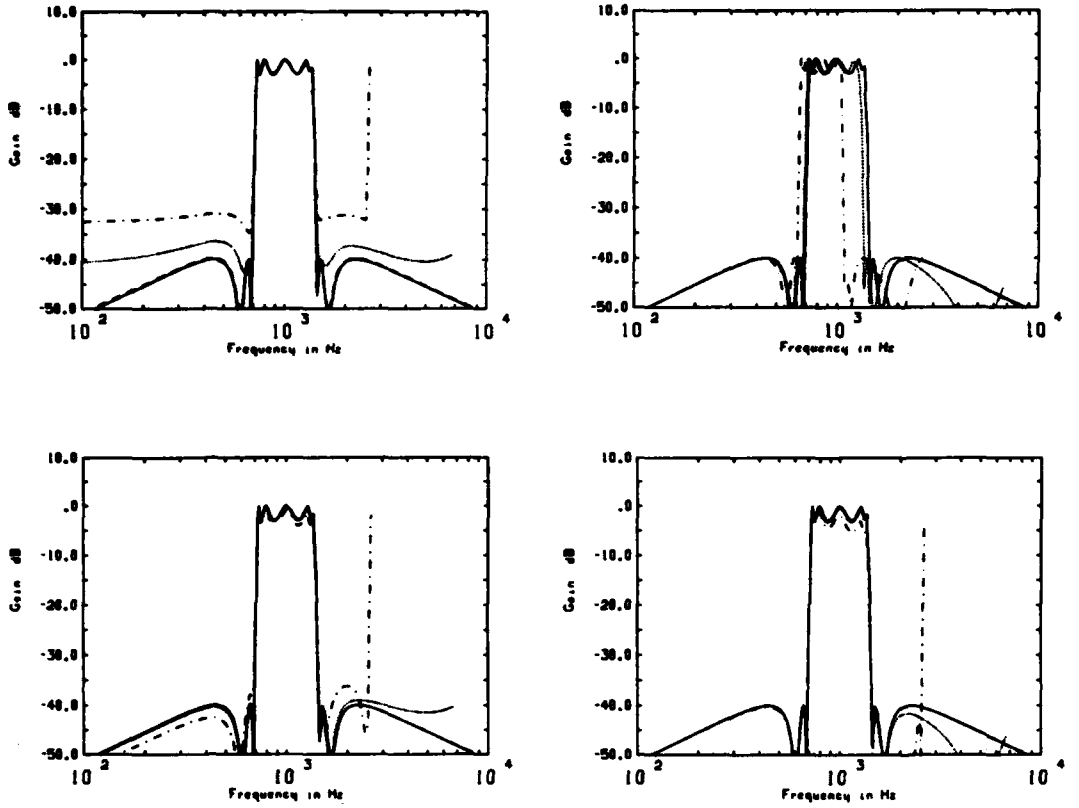

FIGURE 12 - Magnitude response of an elliptic band-pass digital filter obtained by the impulse-invariant, the bilinear, the step- and the ramp-invariant transformations for various sampling frequencies

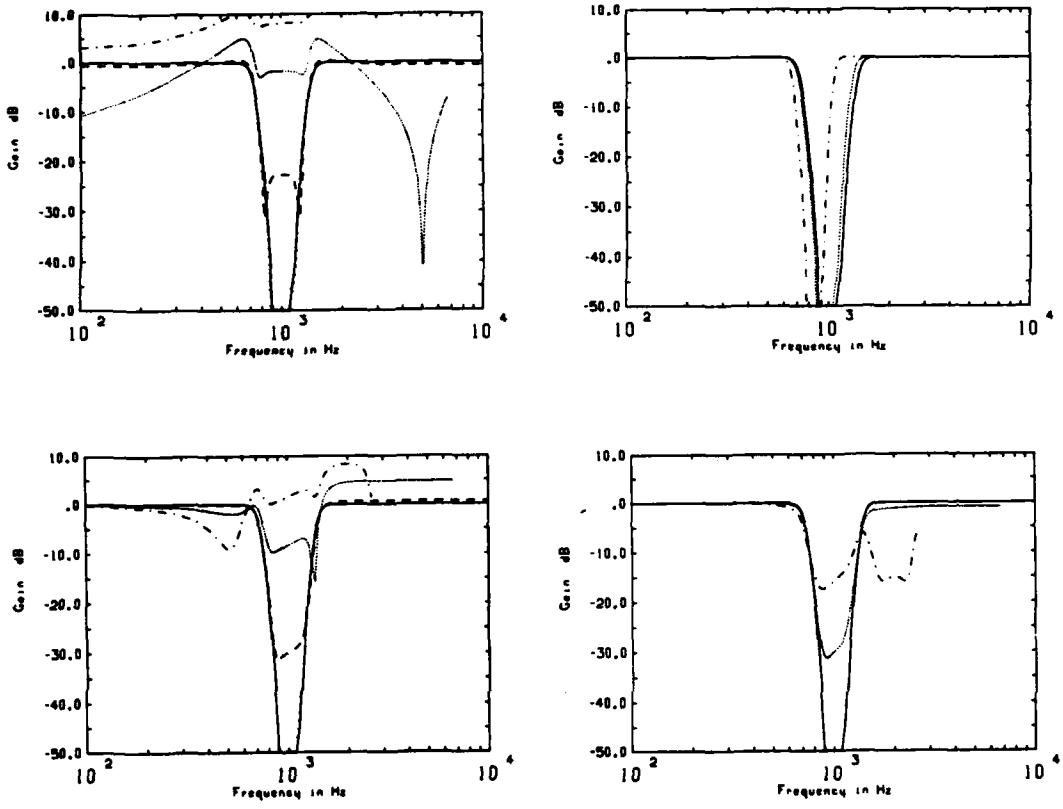

FIGURE 13 - Magnitude response of a Butterworth band-reject digital filter obtained by the impulse-invariant, the bilinear, the step- and the ramp-invariant transformations for various sampling frequencies

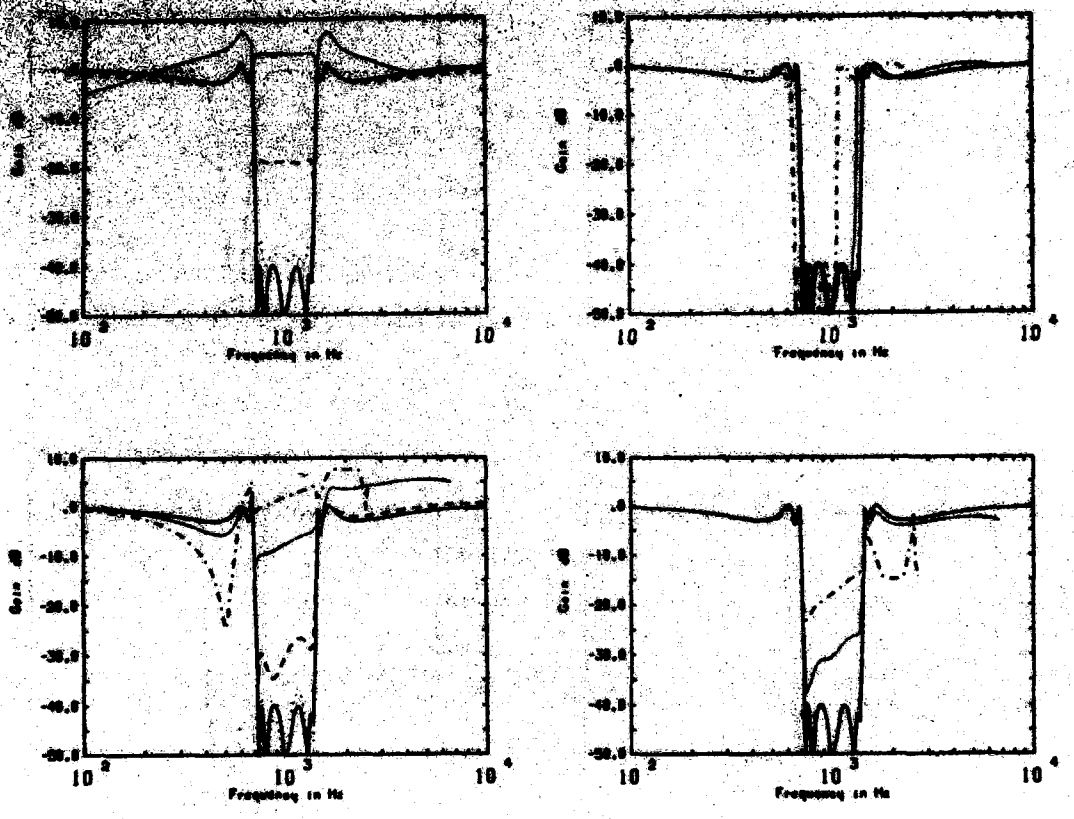

FIGURE 14 - Magnitude response of an elliptic band-reject digital filter obtained by the impulse-invariant, the bilinear, the step- and the ramp-invariant transformations for various sampling frequencies

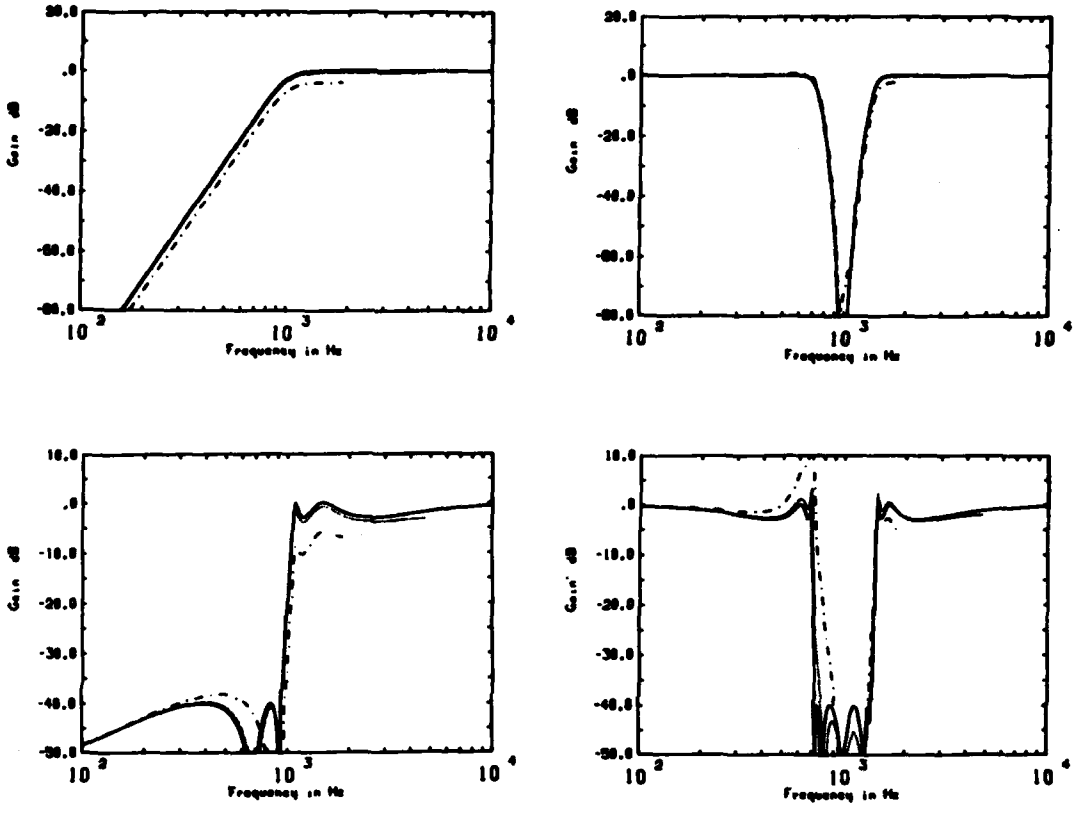

FIGURE 15 - Cascade realization of the ramp-invariance of high-pass and band-reject Butterworth and elliptic filters

7.0 CONCLUSION

Two methods for approximating digital recursive filters from analog filters have been described. The invariant-step response is maintained in one case while the invariant-ramp response is used in the other case. The discrete-time transfer functions of digital filters obtained by these methods were derived for parallel and cascade realizations.

The performance of the proposed methods was first determined by giving the magnitude and phase responses of the first- and second-order filters. It is shown that, for low-pass and band-pass filters, the step-invariant procedure gives accurate magnitude responses that do not vary with the sampling frequency in a frequency band of 0 to $f_s/2$. The ramp invariance gives magnitude responses as accurate as those produced by the step-invariant method for low-pass and band-pass filters and it can be used to reproduce perfectly high-pass filters for ratios f_s/f_p smaller than 10. In addition, a close match in the phase response between the ramp-invariant digital filter and its analog counterpart can be observed for all cases of first- and second-order filters.

Finally, a comparison between the step-, ramp- and impulse-invariant and the bilinear transformations was performed on high-order Butterworth and elliptic filters. At small sampling rates, the impulse-invariant procedure realizes a close match with the analog filter in the magnitude response only for the Butterworth low-pass filter. In the bilinear transformation, the poles of digital filters are moved in relation to the sampling frequency. This distortion, caused by nonlinear frequency warping, becomes significant when the ratio f_s/f_p becomes smaller than 10.

The step and ramp invariance of low-pass and band-pass filters in a parallel implementation produces digital filters whose magnitude response does not depend on the sampling frequency in the frequency band of 0 to $f_s/2$. The magnitude response of the step-invariant high-pass and band-reject filters realized in a parallel or a cascade form is unacceptable for small ratios f_s/f_p (<10). The ramp invariance realized in a cascade form can be used to digitize high-pass and band-reject filters. The ratio f_s/f_p can be decreased to 10 for Butterworth filters but the equiripple character in the stop-band response of elliptic filters is preserved by a ratio f_s/f_p of at least 10.

The step- and ramp-invariant methods are thus less sensitive to frequency folding in comparison with the impulse-invariant method. Furthermore, step invariance can be applied to transfer functions in which the degree of the denominator must exceed that of the numerator by at least one. In the ramp invariance, the numerator degree can be as high as the denominator degree. In addition, when the ramp-invariant transformation is implemented in a parallel form for the low-pass and band-pass filters and in a cascade form for the high-pass and band-reject filters, the resulting match becomes better than the one with the bilinear transformation for ratios f_s/f_p smaller than 10.

8.0 REFERENCES

1. Rabiner, L.R. and Gold, B., "Theory and Application of Digital Signal Processing", Prentice-Hall, Englewood Cliffs, New Jersey, 1975.

2. Oppenheim, A.V. and Schafer, R.W., "Digital Signal Processing", Prentice-Hall, Englewood Cliffs, New Jersey, 1975.

3. Golden, R.M., "Digital Filter Synthesis by Sampled-Data Transformation", IEEE Transactions on Audio and Electroacoustics, Vol. AU-16, No. 3, September 1968.

4. Temes, G.C. and Mitra, S.K., "Modern Filter Theory and Design", John Wiley & Sons, New York, 1973.

5. Antoniou, A., "Digital Filters: Analysis and Design", McGraw-Hill, New York, 1979.

6. Solodovnikov, V.V., "Statistical Dynamics of Linear Automatic Control Systems", translated by W. Chrzczonowicz, D. Van Nostrand Company Ltd., London, 1965.

7. Temes, G.C. and LaPatra, J.W., "Circuit Synthesis and Design", McGraw-Hill, New York, 1977.

APPENDIX A

Representation of the Continuous-Time Transfer Function of Analog Filters

Let us consider that

$$H_A(s) = \frac{Y(s)}{X(s)} = \frac{\sum_{i=0}^{M'} b_i s^i}{\sum_{i=0}^{N'} a_i s^i} \qquad [A.1]$$

is the transfer function of a realizable analog filter if coefficients a_i and b_i are all real, and the degree of the numerator is smaller than or equal to the degree of the denominator.

Equation A.1 can be expanded into partial fractions and, after separating the real from the complex poles, it yields:

$$H(s) = A_0 + \sum_{i=1}^{N} \sum_{k=1}^{M_i} \frac{A_{ik}}{(s + p_i)^k} + \sum_{i=1}^{Nl} \sum_{k=1}^{Ml_i} \frac{B_{2ik}s + B_{1ik}}{(s^2 + 2\alpha_i s + \alpha_i^2 + \beta_i^2)^k} \qquad [A.2]$$

$$H(s) = A_0 + \sum_{i=1}^{N} \sum_{k=1}^{M_i} \frac{A_{ik}}{(s + p_i)^k} + \sum_{i=1}^{Nl} \sum_{k=1}^{Ml_i} \frac{C_{ik}}{(s + d_i)^k} + \frac{C_{ik}^*}{(s + d_i^*)^k} \qquad [A.3]$$

where $C_{ik} = (B_{2ik}/2) + j\,\{(B_{2ik}\alpha_i - B_{1ik})/2\,\beta_i\}$

$d_i = \alpha_i - j\,\beta_i$

The * indicates the complex conjugate. The multiplicity M_i and Ml_i of real poles p_i and complex poles (d_i, d_i^*) are related to the degree of the denominator of H(s) by

$$N' = \sum_{i=1}^{N} M_i + 2\sum_{i=1}^{N1} M1_i \qquad [A.4]$$

If we assume that all real and complex poles are simple, eq. A.3 becomes simply

$$H(s) = A_0 + \sum_{i=1}^{N} \frac{A_i}{s + p_i} + \sum_{i=1}^{N1} \frac{C_i}{s + d_i} + \frac{C_i^*}{s + d_i^*} \qquad [A.5]$$

Equation A.5 covers low-pass, high-pass, band-pass and band-reject filters among the well-known filter classes such as the Butterworth, Bessel, Chebyshev and elliptic filters.

Equations A.2 and A.3 are suitable for representing parallel realization of analog filters. For serial or cascade realization, eq. A.1 must be expressed as

$$H(s) = K_s \frac{\prod_{i=1}^{M'} (s + m_i)}{\prod_{i=1}^{N'} (s + p_i)} \qquad [A.6]$$

If we separate the first- and second-order terms, eq. A.6 becomes

$$H(s) = K_s \left[\prod_{i=1}^{NA} \frac{A_{2i}s + A_{1i}}{s + p_i}\right] \prod_{i=1}^{NB} \frac{B_{5i}s^2 + B_{4i}s + B_{3i}}{s^2 + 2\alpha_i s + \alpha_i^2 + \beta_i^2} \qquad [A.7]$$

where $N' = NA + 2NB$.

Equation A.7 can also be written as

$$H(s) = K_s \left[\prod_{i=1}^{NA} \left(A_{2i} + \frac{A_{1i} - A_{2i}p_i}{s + p_i}\right)\right] \prod_{i=1}^{NB} \left[B_{5i} + \frac{C_{1i}}{s + d_i} + \frac{C_{1i}^*}{s + d_i^*}\right] \qquad [A.8]$$

where

$$c_{11} = \frac{B_{41} - 2\alpha_1 B_{31}}{2} + j \frac{B_{41}\alpha_1 - B_{31} - B_{31}(\alpha_1^2 - \beta_1^2)}{2\beta_1}$$

$$d_1 = \alpha_1 - j\beta_1.$$

APPENDIX B

Realization of the Step- and Ramp-Invariant Digital Filters in a Cascade Form

If the cascade or direct form is desired, it can be obtained by substituting the mapping relations of eqs. 15 and 22 into the transfer functions of analog filters expressed in cascade form (eq. A.8).

For such a realization, the step-invariant transformation becomes

$$S(z) = \left[\prod_{i=1}^{NA} A_{2i} + \frac{\{(A_{1i}/p_i) - A_{2i}\}\ (1 - e^{-p_i T} z^{-1})}{1 - e^{-p_i T} z^{-1}}\right]$$

$$\left[\prod_{i=1}^{NB} B_{5i} + \frac{K_{Ali} z^{-2} + K_{Bli} z^{-1}}{1 - 2e^{-\alpha_i T} \cos \beta_i T z^{-1} + e^{-2\alpha_i T} z^{-2}}\right] \qquad [B.1]$$

where K_{Al} and K_{Bl} are directly obtained by substituting C by C_l in eq. 17 and the ramp invariance becomes

$$R(z) = \prod_{i=1}^{NA} A_{2i} + \frac{A_{1i} - A_{2i} p_i}{1 - e^{-p_i T} z^{-1}} \left[\frac{1 - e^{-p_i T} z^{-1}}{p_i} - \frac{(1 - e^{-p_i T})\ (1 - z^{-1})}{p_i^2 T}\right]$$

$$+ \prod_{i=1}^{NB} B_{5i} + \frac{K_{Cli} + K_{Dli} z^{-1} + K_{Eli} z^{-2}}{1 - 2e^{-\alpha_i T} \cos \beta_i T z^{-1} + e^{-2\alpha_i T} z^{-2}} \qquad [B.2]$$

where K_{Cl}, K_{Dl} and K_{El} are directly obtained by substituting C by C_l in eq. 23.

APPENDIX C

Continuous-Time Transfer Functions of the Butterworth and Elliptic Filters

This appendix gives the continuous-time transfer function of the Butterworth and elliptic filters used in Chapter 8.0.

The transfer function of these filters is written as

$$H(s) = K_s \frac{\prod_{i=1}^{M'} (s + m_i)}{\prod_{i=1}^{N'} (s + p_i)} \qquad [C.1]$$

1) Fifth-order Butterworth low-pass filter:

- cutoff frequency = 1000 Hz
- M' = number of zeros = 0
- N' = number of poles = 5
- $K_s = 9.79 \times 10^{18}$
- $p_{1,2} = 1941 \pm j\ 5975$
  $p_{3,4} = 5083 \pm j\ 3693$
  $p_5 = 6283$

2) Butterworth high-pass filter derived from the low-pass filter:

- cutoff frequency = 1000 Hz
- M' = 5, N' = 5, $K_s = 1$
- poles are identical to those of the low-pass filter
- zeros are all located at 0

3) Butterworth band-pass filter derived from the low-pass filter:

- lower-cutoff frequency = 700 Hz
- upper-cutoff frequency = 1400 Hz
- M' = 5, N' = 10, $K_s = 1.731 \times 10^{18}$
- zeros are all located to 0
- $p_{1,2} = 2221 \pm j\ 5877$
  $p_{3,4} = 1416 \pm j\ 4866$
  $p_{5,6} = 2177 \pm j\ 7478$
  $p_{7,8} = 466.6 \pm j\ 4484$
  $p_{9,10} = 906.3 \pm j\ 8709$

4) Butterworth band-reject filter derived from the low-pass filter:

- lower-cutoff frequency = 700 Hz
- upper-cutoff frequency = 1400 Hz
- M' = 10, N' = 10, $K_s = 1$
- poles are identical to those of the band-pass filter
- 10 zeros are located at $0 \pm j\ 6283$

5) Fifth-order elliptic low-pass filter:

- cutoff frequency = 1000 Hz
- M' = 4, N' = 5, $K_s = 240$
- $m_{1,2} = 0 \pm j\ 9309$, $m_{3,4} = 0 \pm j\ 6865$
- $p_{1,2} = 775.2 \pm j\ 4367$, $p_{3,4} = 155.5 \pm j\ 5802$
  $p_5 = 1479$

6) Elliptic high-pass filter derived from the low-pass filter:

- cutoff frequency = 1000 Hz
- $M' = 5$, $N' = 5$, $K_s = 1$
- $m_{1,2} = 0 \pm j\ 4240$, $m_{3,4} = 0 \pm j\ 5750$
  $m_5 = 0$
- $p_{1,2} = 182.3 \pm j\ 6799$, $p_{3,4} = 1555 \pm j\ 8763$
  $p_5 = 26689$

7) Elliptic band-pass filter derived from the low-pass filter:

- lower-cutoff frequency = 700 Hz
- upper-cutoff frequency = 1400 Hz
- $M' = 9$, $N' = 10$, $K_s = 169.72$
- $m_{1,2} = 0 \pm j\ 10324$, $m_{3,4} = 0 \pm j\ 3801$
  $m_{5,6} = 0 \pm j\ 9163$, $m_{7,8} = 0 \pm j\ 4308$
  $m_9 = 0$
- $p_{1,2} = 379 \pm j\ 4557$, $p_{3,4} = 72.08 \pm j\ 8660$
  $p_{5,6} = 208.6 \pm j\ 4920$, $p_{7,8} = 339.5 \pm j\ 8008$
  $p_{9,10} = 5229 \pm j\ 6261$

8) Elliptic band-reject filter derived from the low-pass filter:

- lower-cutoff frequency = 700 Hz
- upper-cutoff frequency = 1,400 Hz
- $M' = 10$, $N' = 10$, $K_s = 1$
- $m_{1,2} = 0 \pm j\ 6283$, $m_{3,4} = 0 \pm j\ 7959$
  $m_{5,6} = 0 \pm j\ 4960$, $m_{7,8} = 0 \pm j\ 8636$
  $m_{9,10} = 0 \pm j\ 4570$
- $p_1 = 16{,}476$, $p_2 = 2396$
  $p_{3,4} = 41.4 \pm j\ 4323$, $p_{5,6} = 87.4 \pm j\ 9131$
  $p_{7,8} = 306.1 \pm j\ 3889$, $p_{9,10} = 793.7 \pm j\ 10086$

CRDV R-4325/84 (NON CLASSIFIE)

Bureau - Recherche et Développement, MDN, Canada.
CRDV, C.P. 8800, Courcelette, Qué. G0A 1R0

"Dérivation de filtres numériques récursifs par les transformations de l'invariance à l'échelon et l'invariance à la rampe"
par A. Morin et P. Labbé

Ce document décrit deux méthodes pour concevoir des filtres numériques récursifs à partir des filtres analogiques lorsque le rapport entre le taux d'échantillonnage et la fréquence du pôle est faible. Les coefficients des filtres numériques proposés, qui proviennent de l'invariance à l'échelon et à la rampe des filtres analogiques correspondants, ont été déterminés pour les pôles réels et complexes. Pour les filtres d'ordres plus élevés réalisés dans un réseau parallèle, il est démontré que la fonction de transfert en z des filtres numériques caractérisés par l'invariance à l'échelon et à la rampe peut être déduite directement de la transformée en z ou de la décomposition en fractions partielles de la fonction de transfert des filtres analogiques. On a aussi déduit la fonction de transfert en z des filtres invariants à l'échelon et à la rampe pour une réalisation dans un réseau en série. Finalement, la performance de ces méthodes est démontré en traçant les réponses en amplitude et en phase des filtres numériques du premier et du deuxième ordre. Pour des filtres Butterworth et elliptiques d'ordres élevés, on compare la réponse en amplitude des filtres invariants à l'échelon et à la rampe avec celle obtenue par des méthodes courantes telles que la transformée en z et la transformée bilinéaire.

CRDV R-4325/84 (NON CLASSIFIE)

Bureau - Recherche et Développement, MDN, Canada.
CRDV, C.P. 8800, Courcelette, Qué. G0A 1R0

"Dérivation de filtres numériques récursifs par les transformations de l'invariance à l'échelon et l'invariance à la rampe"
par A. Morin et P. Labbé

Ce document décrit deux méthodes pour concevoir des filtres numériques récursifs à partir des filtres analogiques lorsque le rapport entre le taux d'échantillonnage et la fréquence du pôle est faible. Les coefficients des filtres numériques proposés, qui proviennent de l'invariance à l'échelon et à la rampe des filtres analogiques correspondants, ont été déterminés pour les pôles réels et complexes. Pour les filtres d'ordres plus élevés réalisés dans un réseau parallèle, il est démontré que la fonction de transfert en z des filtres numériques caractérisés par l'invariance à l'échelon et à la rampe peut être déduite directement de la transformée en z ou de la décomposition en fractions partielles de la fonction de transfert des filtres analogiques. On a aussi déduit la fonction de transfert en z des filtres invariants à l'échelon et à la rampe pour une réalisation dans un réseau en série. Finalement, la performance de ces méthodes est démontré en traçant les réponses en amplitude et en phase des filtres numériques du premier et du deuxième ordre. Pour des filtres Butterworth et elliptiques d'ordres élevés, on compare la réponse en amplitude des filtres invariants à l'échelon et à la rampe avec celle obtenue par des méthodes courantes telles que la transformée en z et la transformée bilinéaire.

CRDV R-4325/84 (NON CLASSIFIE)

Bureau - Recherche et Développement, MDN, Canada.
CRDV, C.P. 8800, Courcelette, Qué. G0A 1R0

"Dérivation de filtres numériques récursifs par les transformations de l'invariance à l'échelon et l'invariance à la rampe"
par A. Morin et P. Labbé

Ce document décrit deux méthodes pour concevoir des filtres numériques récursifs à partir des filtres analogiques lorsque le rapport entre le taux d'échantillonnage et la fréquence du pôle est faible. Les coefficients des filtres numériques proposés, qui proviennent de l'invariance à l'échelon et à la rampe des filtres analogiques correspondants, ont été déterminés pour les pôles réels et complexes. Pour les filtres d'ordres plus élevés réalisés dans un réseau parallèle, il est démontré que la fonction de transfert en z des filtres numériques caractérisés par l'invariance à l'échelon et à la rampe peut être déduite directement de la transformée en z ou de la décomposition en fractions partielles de la fonction de transfert des filtres analogiques. On a aussi déduit la fonction de transfert en z des filtres invariants à l'échelon et à la rampe pour une réalisation dans un réseau en série. Finalement, la performance de ces méthodes est démontré en traçant les réponses en amplitude et en phase des filtres numériques du premier et du deuxième ordre. Pour des filtres Butterworth et elliptiques d'ordres élevés, on compare la réponse en amplitude des filtres invariants à l'échelon et à la rampe avec celle obtenue par des méthodes courantes telles que la transformée en z et la transformée bilinéaire.

CRDV R-4325/84 (NON CLASSIFIE)

Bureau - Recherche et Développement, MDN, Canada.
CRDV, C.P. 8800, Courcelette, Qué. G0A 1R0

"Dérivation de filtres numériques récursifs par les transformations de l'invariance à l'échelon et l'invariance à la rampe"
par A. Morin et P. Labbé

Ce document décrit deux méthodes pour concevoir des filtres numériques récursifs à partir des filtres analogiques lorsque le rapport entre le taux d'échantillonnage et la fréquence du pôle est faible. Les coefficients des filtres numériques proposés, qui proviennent de l'invariance à l'échelon et à la rampe des filtres analogiques correspondants, ont été déterminés pour les pôles réels et complexes. Pour les filtres d'ordres plus élevés réalisés dans un réseau parallèle, il est démontré que la fonction de transfert en z des filtres numériques caractérisés par l'invariance à l'échelon et à la rampe peut être déduite directement de la transformée en z ou de la décomposition en fractions partielles de la fonction de transfert des filtres analogiques. On a aussi déduit la fonction de transfert en z des filtres invariants à l'échelon et à la rampe pour une réalisation dans un réseau en série. Finalement, la performance de ces méthodes est démontré en traçant les réponses en amplitude et en phase des filtres numériques du premier et du deuxième ordre. Pour des filtres Butterworth et elliptiques d'ordres élevés, on compare la réponse en amplitude des filtres invariants à l'échelon et à la rampe avec celle obtenue par des méthodes courantes telles que la transformée en z et la transformée bilinéaire.

DREV R-4325/84 (UNCLASSIFIED)

Research and Development Branch, DND, Canada.
DREV, P.O. Box 8800, Courcelette, Que. G0A 1R0

"Derivation of Recursive Digital Filters by the Step-Invariant and the Ramp-Invariant Transformations"
by A. Morin and P. Labbé

This document describes two procedures for designing recursive digital filters from continuous-time filters when the ratio of the sampling frequency to the pole frequency is small. The coefficients of the proposed digital filters, which are derived from the step and ramp invariance of the corresponding analog filters, have been determined for real and complex poles. For higher-order filters realised in a parallel form, it is demonstrated that the discrete-time transfer function of digital filters obtained by the step and ramp invariance can be derived directly from the standard z-transformation or from the partial fraction expansion of the continuous-time transfer function. The discrete-time transfer functions of the step- and ramp-invariant filters realised in a cascade form have also been derived. Finally, the performance of these methods is demonstrated by plotting the magnitude and phase responses of the first- and second-order digital filters. For high-order Butterworth and elliptic filters, the magnitude responses of step-invariant and ramp-invariant filters are compared with those obtained by usual methods such as the standard z and the bilinear transformations.

DREV R-4325/84 (UNCLASSIFIED)

Research and Development Branch, DND, Canada.
DREV, P.O. Box 8800, Courcelette, Que. G0A 1R0

"Derivation of Recursive Digital Filters by the Step-Invariant and the Ramp-Invariant Transformations"
by A. Morin and P. Labbé

This document describes two procedures for designing recursive digital filters from continuous-time filters when the ratio of the sampling frequency to the pole frequency is small. The coefficients of the proposed digital filters, which are derived from the step and ramp invariance of the corresponding analog filters, have been determined for real and complex poles. For higher-order filters realised in a parallel form, it is demonstrated that the discrete-time transfer function of digital filters obtained by the step and ramp invariance can be derived directly from the standard z-transformation or from the partial fraction expansion of the continuous-time transfer function. The discrete-time transfer functions of the step- and ramp-invariant filters realised in a cascade form have also been derived. Finally, the performance of these methods is demonstrated by plotting the magnitude and phase responses of the first- and second-order digital filters. For high-order Butterworth and elliptic filters, the magnitude responses of step-invariant and ramp-invariant filters are compared with those obtained by usual methods such as the standard z and the bilinear transformations.

DREV R-4325/84 (UNCLASSIFIED)

Research and Development Branch, DND, Canada.
DREV, P.O. Box 8800, Courcelette, Que. G0A 1R0

"Derivation of Recursive Digital Filters by the Step-Invariant and the Ramp-Invariant Transformations"
by A. Morin and P. Labbé

This document describes two procedures for designing recursive digital filters from continuous-time filters when the ratio of the sampling frequency to the pole frequency is small. The coefficients of the proposed digital filters, which are derived from the step and ramp invariance of the corresponding analog filters, have been determined for real and complex poles. For higher-order filters realised in a parallel form, it is demonstrated that the discrete-time transfer function of digital filters obtained by the step and ramp invariance can be derived directly from the standard z-transformation or from the partial fraction expansion of the continuous-time transfer function. The discrete-time transfer functions of the step- and ramp-invariant filters realised in a cascade form have also been derived. Finally, the performance of these methods is demonstrated by plotting the magnitude and phase responses of the first- and second-order digital filters. For high-order Butterworth and elliptic filters, the magnitude responses of step-invariant and ramp-invariant filters are compared with those obtained by usual methods such as the standard z and the bilinear transformations.

DREV R-4325/84 (UNCLASSIFIED)

Research and Development Branch, DND, Canada.
DREV, P.O. Box 8800, Courcelette, Que. G0A 1R0

"Derivation of Recursive Digital Filters by the Step-Invariant and the Ramp-Invariant Transformations"
by A. Morin and P. Labbé

This document describes two procedures for designing recursive digital filters from continuous-time filters when the ratio of the sampling frequency to the pole frequency is small. The coefficients of the proposed digital filters, which are derived from the step and ramp invariance of the corresponding analog filters, have been determined for real and complex poles. For higher-order filters realised in a parallel form, it is demonstrated that the discrete-time transfer function of digital filters obtained by the step and ramp invariance can be derived directly from the standard z-transformation or from the partial fraction expansion of the continuous-time transfer function. The discrete-time transfer functions of the step- and ramp-invariant filters realised in a cascade form have also been derived. Finally, the performance of these methods is demonstrated by plotting the magnitude and phase responses of the first- and second-order digital filters. For high-order Butterworth and elliptic filters, the magnitude responses of step-invariant and ramp-invariant filters are compared with those obtained by usual methods such as the standard z and the bilinear transformations.

END

FILMED

11-84

DTIC